



Near-threshold $D\bar{D}$ spectroscopy and observation of a new charmonium state

LHCb collaboration[†]

Abstract

Using proton-proton collision data, corresponding to an integrated luminosity of 9fb^{-1} , collected with the LHCb detector between 2011 and 2018, a new narrow charmonium state, the X(3842) resonance, is observed in the decay modes $X(3842) \rightarrow D^0\bar{D}^0$ and $X(3842) \rightarrow D^+D^-$. The mass and the natural width of this state are measured to be

$$\begin{aligned} m_{X(3842)} &= 3842.71 \pm 0.16 \pm 0.12 \text{ MeV}/c^2, \\ \Gamma_{X(3842)} &= 2.79 \pm 0.51 \pm 0.35 \text{ MeV}, \end{aligned}$$

where the first uncertainty is statistical and the second is systematic. The observed mass and narrow natural width suggest the interpretation of the new state as the unobserved spin-3 $\psi_3(1^3D_3)$ charmonium state.

In addition, prompt hadroproduction of the $\psi(3770)$ and $\chi_{c2}(3930)$ states is observed for the first time, and the parameters of these states are measured to be

$$\begin{aligned} m_{\psi(3770)} &= 3778.1 \pm 0.7 \pm 0.6 \text{ MeV}/c^2, \\ m_{\chi_{c2}(3930)} &= 3921.9 \pm 0.6 \pm 0.2 \text{ MeV}/c^2, \\ \Gamma_{\chi_{c2}(3930)} &= 36.6 \pm 1.9 \pm 0.9 \text{ MeV}, \end{aligned}$$

where the first uncertainty is statistical and the second is systematic.

Published in JHEP 1907 (2019) 035

© 2019 CERN for the benefit of the LHCb collaboration. CC-BY-4.0 licence.

[†]Authors are listed at the end of this paper.

1 Introduction

Since the discovery of the J/ψ resonance in 1974 [1, 2], the spectrum of hidden charm mesons has been mapped out experimentally with high precision. Theoretically, the spectra and properties of these states are well described by potential models [3]. In recent years, there has been a revival of interest in charmonium spectroscopy initially triggered by the discovery of the $\chi_{c1}(3872)$ meson¹ by the Belle experiment [4] and the subsequent observation of other states that do not fit into the conventional hidden-charm spectrum. To be confident that the new states are exotic in nature, all predicted $c\bar{c}$ states need to be accounted for.

Amongst the expected charmonia close to $D\bar{D}$ threshold, the states $\eta_{c2}(1^1D_2)$ and $\psi_3(1^3D_3)$ remain undiscovered [5, 6]. Though the latter state lies above the open charm threshold, the decay to the $D\bar{D}$ final state is suppressed due to the F-wave centrifugal barrier factor. Consequently, the $\psi_3(1^3D_3)$ state is expected to be narrow with a natural width of 1–2 MeV [7, 8]. Predictions for the mass of this state lie in the range 3815–3863 MeV/ c^2 [6, 9–15]. Since it has negative C parity, it cannot be produced in either $\gamma\gamma$ annihilation or gg fusion. In Ref. [8] it is suggested that a possible production mechanism for this state is via electric-dipole radiative transitions from the $\chi_{c2}(2^3P_2)$ tensor state.

In this paper, the observation of a new $c\bar{c}$ meson decaying to both the D^+D^- and $D^0\bar{D}^0$ final states is reported. The data sample used for this analysis corresponds to an integrated luminosity of 9 fb^{-1} recorded with the LHCb detector in pp collisions at centre-of-mass energies of 7, 8 and 13 TeV, during the years 2011–2018. The mass and width of the new state are quite similar to those expected for the missing $\psi_3(1^3D_3)$ state with $J^{PC} = 3^{--}$. In addition, the production of both $\psi(3770)$ and $\chi_{c2}(3930)$ mesons is observed. The first state is well known through measurements at e^+e^- colliders, but so far it has only been observed in a hadronic environment in the $\mu^+\mu^-$ mass spectrum of $B^+ \rightarrow K^+\mu^+\mu^-$ decays² [16]. The latter state has only been previously observed in the $\gamma\gamma \rightarrow D\bar{D}$ process by the Belle and BaBar experiments [17, 18]. Both analyses prefer a spin assignment of 2 for this state based upon one-dimensional angular distributions.

2 The LHCb detector and simulation

The LHCb detector [19, 20] is a single-arm forward spectrometer covering the pseudorapidity range $2 < \eta < 5$, designed for the study of particles containing b or c quarks. The detector includes a high-precision tracking system consisting of a silicon-strip vertex detector surrounding the pp interaction region [21], a large-area silicon-strip detector located upstream of a dipole magnet with a bending power of about 4 Tm, and three stations of silicon-strip detectors and straw drift tubes [22, 23] placed downstream of the magnet. The tracking system provides a measurement of the momentum, p , of charged particles with a relative uncertainty that varies from 0.5% at low momentum to 1.0% at 200 GeV/ c . The momentum scale is calibrated using samples of $J/\psi \rightarrow \mu^+\mu^-$ and $B^+ \rightarrow J/\psi K^+$ decays collected concurrently with the data sample used for this analysis [24, 25]. The relative accuracy of this procedure is estimated to be 3×10^{-4} using samples

¹Also known as the X(3872) state.

²The inclusion of charge-conjugate processes is implied throughout the paper.

of other fully reconstructed b hadrons, Υ and K_S^0 mesons. The minimum distance of a track to a primary vertex (PV), the impact parameter (IP), is measured with a resolution of $(15 + 29/p_T) \mu\text{m}$, where p_T is the component of the momentum transverse to the beam, in GeV/c . Different types of charged hadrons are distinguished using information from two ring-imaging Cherenkov detectors (RICH) [26]. Photons, electrons and hadrons are identified by a calorimeter system consisting of scintillating-pad and preshower detectors, an electromagnetic and a hadronic calorimeter. Muons are identified by a system composed of alternating layers of iron and multiwire proportional chambers [27].

The online event selection is performed by a trigger [28], which consists of a hardware stage, based on information from the calorimeter and muon systems, followed by a software stage, which applies a full event reconstruction. At the hardware trigger stage, events are required to have a muon with high p_T or a hadron, photon or electron with high transverse energy in the calorimeters. The software trigger requires a two-, three- or four-track secondary vertex with a significant displacement from any primary pp interaction vertex. At least one charged particle must have transverse momentum $p_T > 1.6 \text{ GeV}/c$ and be inconsistent with originating from a PV.

The analysis procedure is validated using a simulation in which pp collisions are generated using PYTHIA [29] with a specific LHCb configuration [30]. Decays of unstable particles are described by EVTGEN [31], in which final-state radiation is generated using PHOTOS [32]. The interaction of the generated particles with the detector, and its response, are implemented using the GEANT4 toolkit [33] as described in Ref. [34].

3 Selection

The criteria used to select D^0 and D^+ candidates are similar to those described in Refs. [35–37]. The selection starts from good-quality charged tracks with $p_T > 250 \text{ MeV}/c$ that are inconsistent with being produced in a pp interaction vertex. Selected tracks are required to be identified as either kaons or pions using information from the RICH detectors, and are then used to build D^0 and D^+ candidates reconstructed in the $D^0 \rightarrow K^-\pi^+$ and $D^+ \rightarrow K^-\pi^+\pi^+$ decay modes. The tracks forming D^0 and D^+ candidates are required to originate from a common vertex. To reduce combinatorial background, the decay time of D^0 and D^+ candidates is required to exceed $100 \mu\text{m}/c$ and the momentum direction to be consistent with the vector from the primary to the secondary vertex. The latter requirement also reduces the contribution from charm hadrons produced in the weak decays of long-lived beauty hadrons. Selected D^0 and D^+ candidates, generically referred to as D candidates hereafter, with $p_T > 1 \text{ GeV}/c$ are combined to form $D^0\bar{D}^0$ and D^+D^- candidates. A fit is performed for each $D\bar{D}$ candidate [38], such that both D mesons are required to originate from a common vertex that is consistent with the PV location. A requirement on the fit χ^2 reduces, to a negligible level, the background from D and \bar{D} candidates produced in two independent pp interactions, and further suppresses the contribution from beauty hadrons.

The two-dimensional distributions for the D and \bar{D} masses are shown in Fig. 1. Only D candidates with mass within $\pm 20 \text{ MeV}/c^2$ (approximately $\pm 3\sigma$) of the known D-meson masses [39] are kept for subsequent analysis. The purity of the selected samples is 88% and 83% for the $D^0\bar{D}^0$ and D^+D^- modes, respectively.

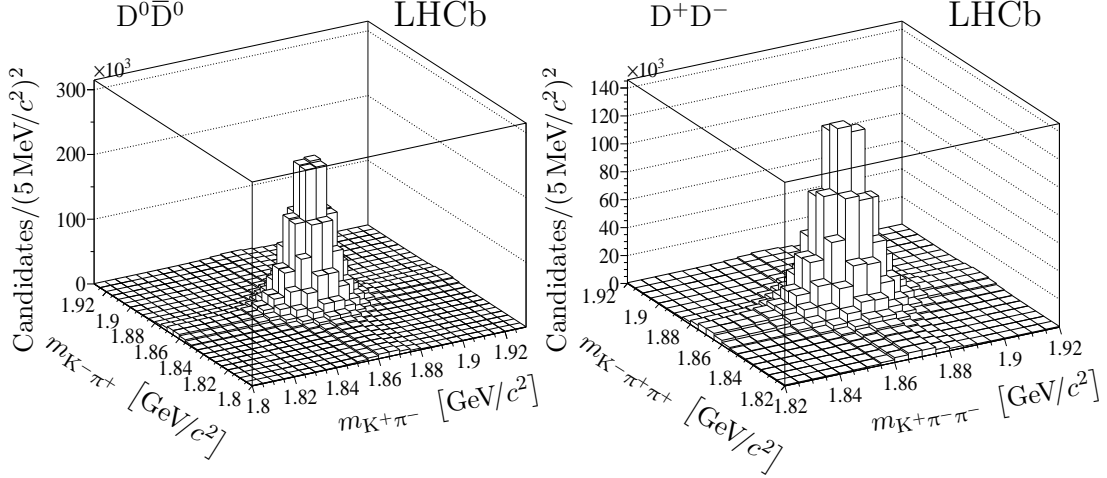


Figure 1: Distributions of (left) $m_{K^- \pi^+}$ versus $m_{K^+ \pi^-}$ and (right) $m_{K^- \pi^+ \pi^+}$ versus $m_{K^+ \pi^- \pi^-}$ for selected DD candidates.

4 DD mass spectra

To improve the $D\bar{D}$ mass resolution, a new fit [38] is performed with the masses of both D candidates constrained to the known values [39]. After this fit, the $D\bar{D}$ mass spectra for selected $D^0\bar{D}^0$ and D^+D^- pairs close to the $D\bar{D}$ threshold with $m_{D\bar{D}} < 4.2 \text{ GeV}/c^2$ are shown in Fig. 2. Four peaking structures are seen:

- A narrow peak in the $D^0\bar{D}^0$ spectrum just above the threshold, interpreted as the $\chi_{c1}(3872) \rightarrow D^{*0}\bar{D}^0$ decay, followed by $D^{*0} \rightarrow D^0\pi^0$ or $D^{*0} \rightarrow D^0\gamma$ — due to the small energy release in this decay, the mass of the $D\bar{D}$ pair gives a narrow peak in the $D^0\bar{D}^0$ mass spectrum at the $D^0\bar{D}^0$ threshold;
- A broad peak close to $3780 \text{ MeV}/c^2$, visible both in $D^0\bar{D}^0$ and D^+D^- mass spectra and associated with the contribution from $\psi(3770) \rightarrow D\bar{D}$ decays;
- A very narrow peak at $m_{D\bar{D}} \approx 3840 \text{ MeV}/c^2$, referred to hereafter as X(3842);
- A wide structure in the D^+D^- mass spectrum at $m_{D^+D^-} \approx 3920 \text{ MeV}/c^2$ also visible in the $D^0\bar{D}^0$ mass spectrum and interpreted to be due to $\chi_{c2}(3930) \rightarrow DD$ decays.

To better parameterise the background, fits to the $D\bar{D}$ mass spectra are performed separately in three different overlapping mass regions: a narrow region $3.80 < m_{D\bar{D}} < 3.88 \text{ GeV}/c^2$ around the X(3842) peak; the high-mass region $3.8 < m_{D\bar{D}} < 4.2 \text{ GeV}/c^2$ and the near-threshold region $m_{D\bar{D}} < 3.88 \text{ GeV}/c^2$.

4.1 Mass region $3.80 < m_{D\bar{D}} < 3.88 \text{ GeV}/c^2$

The narrow natural width and the mass of the X(3842) state suggest the interpretation of the X(3842) state as the $\psi_3(1^3D_3)$ charmonium state with $J^{PC} = 3^{--}$ [8]. The X(3842) signal is modelled by a relativistic Breit–Wigner function with Blatt–Weisskopf form factors [40]. The orbital angular momentum between the D and \bar{D} mesons is assumed to be $L = 3$. Alternative hypotheses for the spin assignment are discussed in Sect. 5.

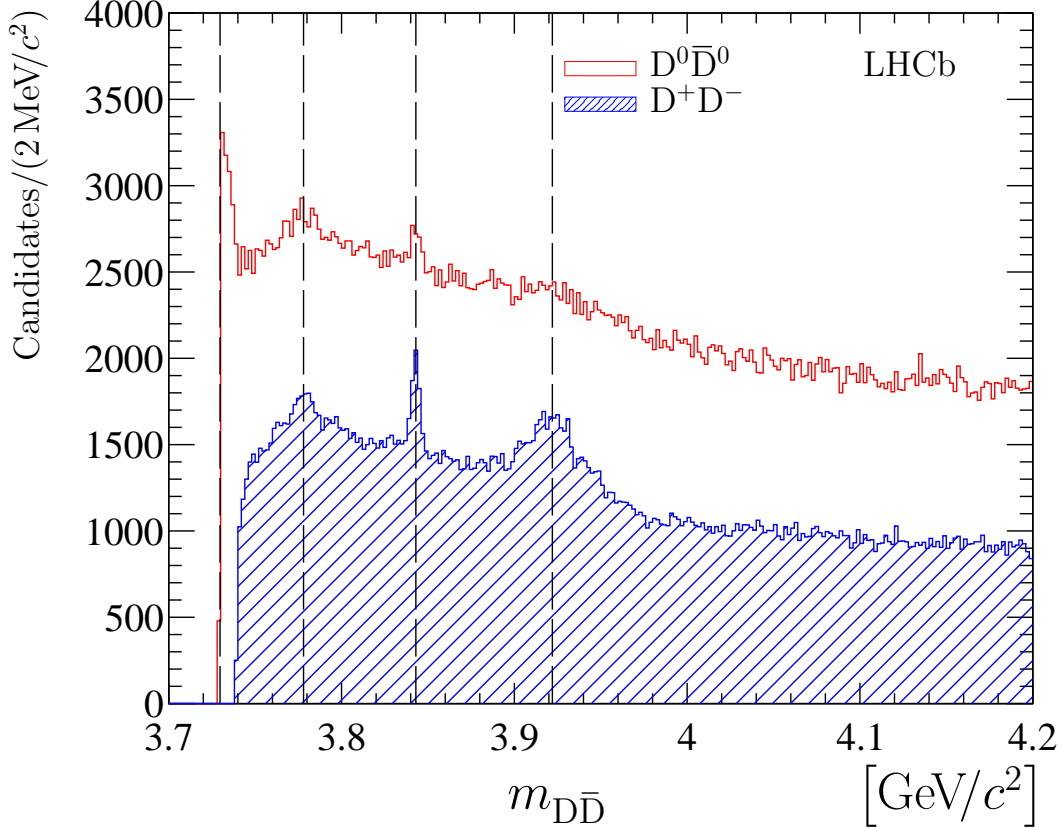


Figure 2: The mass spectra for selected $D\bar{D}$ combinations. The open red histogram corresponds to $D^0\bar{D}^0$ pairs, while the hatched blue histogram corresponds to D^+D^- pairs. Vertical black dashed lines help to identify the peaks from (left to right) $\chi_{c1}(3872) \rightarrow D^{*0}\bar{D}^0$, $\psi(3770) \rightarrow D\bar{D}$, $X(3842) \rightarrow D\bar{D}$ and $\chi_{c2}(3930) \rightarrow D\bar{D}$ decays.

The relativistic Breit–Wigner function is convolved with the detector resolution, described by a sum of two Gaussian functions with common mean and parameters fixed from simulation. The effective resolution depends on $m_{D^+D^-}$ and increases from $0.9 \text{ MeV}/c^2$ for $\psi(3770) \rightarrow D^+D^-$ to $1.9 \text{ MeV}/c^2$ for $\chi_{c2}(3930) \rightarrow D^+D^-$ signals and is approximately 10% larger for the $D^0\bar{D}^0$ final state. The background in this region is found to be well described by a second-order polynomial function.

An extended unbinned maximum-likelihood fit is performed simultaneously to the $D^0\bar{D}^0$ and D^+D^- mass spectra. The mass and the natural width of the $X(3842)$ signals in the $D^0\bar{D}^0$ and D^+D^- final state are considered as common parameters in this fit whilst all other parameters are allowed to vary independently. All parameters related to the detector resolution are fixed to values found using simulation. The result of the fit to the data is shown in Fig. 3 and the resulting parameters of interest are summarised in Table 1. The statistical significance of the $X(3842)$ signal is evaluated using Wilks’ theorem [41] to be above 7σ for the $D^0\bar{D}^0$ decay mode and above 21σ for the D^+D^- decay mode.

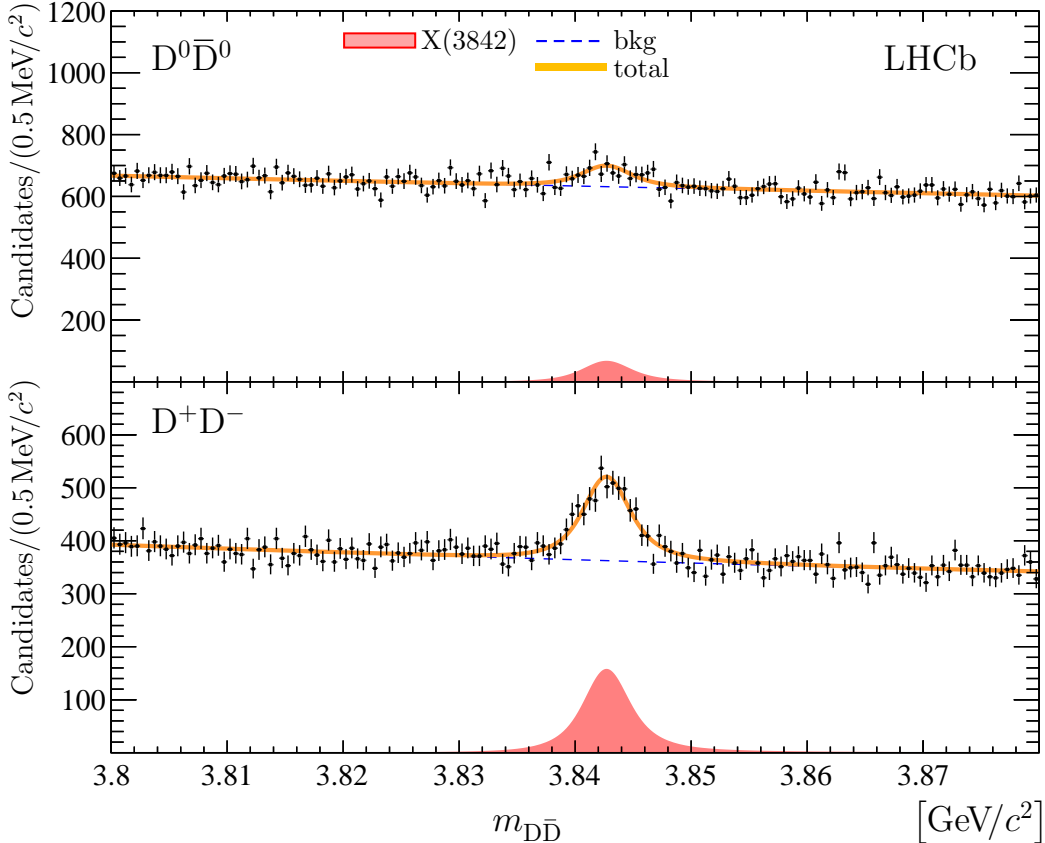


Figure 3: Mass spectra of (top) $D^0\bar{D}^0$ and (bottom) D^+D^- candidates in the narrow $3.80 < m_{D\bar{D}} < 3.88 \text{ GeV}/c^2$ region. The result of the simultaneous fit described in the text is superimposed.

Table 1: Yields, mass and width of the X(3842) state from the fit to $D\bar{D}$ mass spectra in the narrow $3.80 < m_{D\bar{D}} < 3.88 \text{ GeV}/c^2$ region. Uncertainties are statistical only.

	$N_{X(3842)}$	$m_{X(3842)} [\text{MeV}/c^2]$	$\Gamma_{X(3842)} [\text{MeV}]$
$D^0\bar{D}^0$	930 ± 170	3842.71 ± 0.16	2.79 ± 0.51
D^+D^-	2070 ± 190		

4.2 Mass region $3.80 < m_{D\bar{D}} < 4.20 \text{ GeV}/c^2$

Two signal components are used to describe the $3.80 < m_{D\bar{D}} < 4.20 \text{ GeV}/c^2$ region: the X(3842) component, described earlier, and a component for the $\chi_{c2}(3930)$ decay, modelled by the convolution of a relativistic D-wave Breit–Wigner function with the resolution model described above. The background in this mass region is modelled by an exponential function multiplied by a second-order polynomial function. The total fit consists of the sum of the background and the X(3842) and $\chi_{c2}(3930)$ signals. A simultaneous extended binned maximum-likelihood fit to the $D^0\bar{D}^0$ and D^+D^- mass spectra is performed with the mass and natural width of the X(3842) state fixed to the results of the

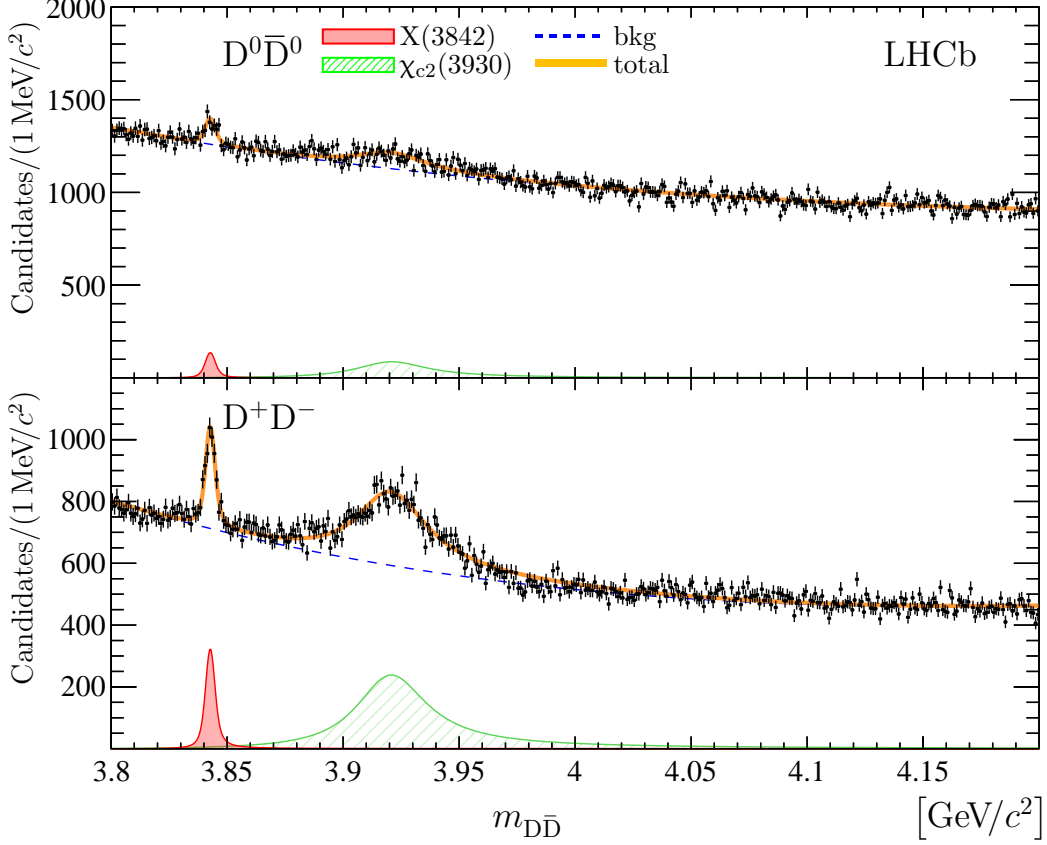


Figure 4: Mass spectra of (top) $D^0\bar{D}^0$ and (bottom) D^+D^- candidates in the high-mass $3.80 < m_{D\bar{D}} < 4.20 \text{ GeV}/c^2$ region. The result of the simultaneous fit described in the text is superimposed.

fit in the narrow $3.80 < m_{D\bar{D}} < 3.88 \text{ GeV}/c^2$ region. The mass and the natural width of the $\chi_{c2}(3930)$ signals in the $D^0\bar{D}^0$ and D^+D^- final states and the slope of the background exponential function are common parameters and all other parameters are allowed to vary independently. The result of the fit of this model to the data is shown in Fig. 4 and the resulting parameters of interest are summarised in Table 2. If the wide peak in Fig. 4 is instead assumed to be spin-0 then the mass decreases by $0.12 \text{ MeV}/c^2$ while variations in the width and the uncertainties in the mass and width are negligible.

Table 2: Yields, mass and width of the $\chi_{c2}(3920)$ state from the fit to $D\bar{D}$ mass spectra in the high-mass $3.88 < m_{D\bar{D}} < 4.20 \text{ GeV}/c^2$ region. Uncertainties are statistical only.

	$N_{\chi_{c2}(3930)}$ [10^3]	$m_{\chi_{c2}(3930)}$ [MeV/c^2]	$\Gamma_{\chi_{c2}(3930)}$ [MeV]
$D^0\bar{D}^0$	4.7 ± 0.5	3921.90 ± 0.55	36.64 ± 1.88
D^+D^-	13.0 ± 0.6		

Table 3: Yields and mass of the $\psi(3770)$ state from the fit to $D\bar{D}$ mass spectra in the near-threshold $m_{D\bar{D}} < 3.88 \text{ GeV}/c^2$ region. Uncertainties are statistical only.

	$N_{\psi(3770)}$ [10^3]	$m_{\psi(3770)}$ [MeV/c^2]
$D^0\bar{D}^0$	5.1 ± 0.5	3778.13 ± 0.70
D^+D^-	5.7 ± 0.4	

4.3 Mass region $m_{D\bar{D}} < 3.88 \text{ GeV}/c^2$

To fit the $D\bar{D}$ mass spectra in the near-threshold region, $m_{D\bar{D}} < 3.88 \text{ GeV}/c^2$, components for the $X(3842)$ and $\psi(3770)$ decays to $D\bar{D}$ signals and the background are included. In the case of the $D^0\bar{D}^0$ mass spectrum, an additional contribution from $\chi_{c1}(3872) \rightarrow D^{*0}\bar{D}^0$ decays followed by $D^{*0} \rightarrow D^0\pi^0$ or $D^{*0} \rightarrow D^0\gamma$ is required. The $\psi(3770) \rightarrow D\bar{D}$ component is modelled as a relativistic multi-channel P-wave Breit–Wigner function [42, 43], accounting for decays into $D^0\bar{D}^0$, D^+D^- and non- $D\bar{D}$ final states [39], convolved with a double-Gaussian resolution model. The background is modelled as a product of a scaled two-body phase-space function and a second-order polynomial function. The shape of the feed-down contribution from $\chi_{c1}(3872)$ decays is described using simulated two-body $\chi_{c1}(3872) \rightarrow D^{*0}\bar{D}^0$ and three-body $\chi_{c1}(3872) \rightarrow D^0\bar{D}^0\pi^0$ decays. The latter corresponds to off-shell decays of the intermediate D^{*0} mesons [44, 45]. The simulation of $\chi_{c1}(3872) \rightarrow D^{*0}\bar{D}^0$ decays assumes that the D^{*0} mesons are unpolarised and the three-body decay dynamics are not included. The contributions from the two-body and three-body decays of the $\chi_{c1}(3872)$ state are allowed to vary independently in the fit.

A simultaneous binned extended maximum-likelihood fit to the $D^0\bar{D}^0$ and D^+D^- mass spectra is performed. In this fit, the mass and width of the $X(3842)$ signal are fixed from the results of the unbinned fit in the narrow $3.80 < m(D\bar{D}) < 3.88 \text{ GeV}/c^2$ region, the mass of the $\psi(3770)$ state is allowed to vary, while the natural width of the $\psi(3770)$ state is Gaussian-constrained to the known value of $\Gamma_{\psi(3770)} = 27.2 \pm 1.0 \text{ MeV}$ [39]. The mass of the $\psi(3770)$ state and the scale factor for the background two-body phase space function are common parameters and all other parameters are allowed to vary independently. The result of the fit to the $D^0\bar{D}^0$ and D^+D^- mass spectra is shown in Fig. 5 and the resulting parameters of interest are summarised in Table 3. The fit quality in the region $m_{D^0\bar{D}^0} < 3.74 \text{ GeV}/c^2$ is poor, possibly due to large effects of the neglected dynamics in $\chi_{c1}(3872) \rightarrow D^0\bar{D}^0X$ decays. However, it is found that the exact description of the $\chi_{c1}(3872)$ contribution does not affect the measurement of the mass of the $\psi(3770)$ state.

5 Systematic uncertainties

In the proximity of the $D\bar{D}$ mass threshold most potential systematic uncertainties for the mass and natural width measurements become negligible when D mass constraints are applied. The main systematic uncertainties for the measured $X(3842)$, $\chi_{c2}(3930)$ and $\psi(3770)$ resonance parameters are related to the signal and background parameterisation, the momentum-scale calibration and the uncertainty in the known D^0 and D^+ masses [39]. These are described below and summarised in Table 4.

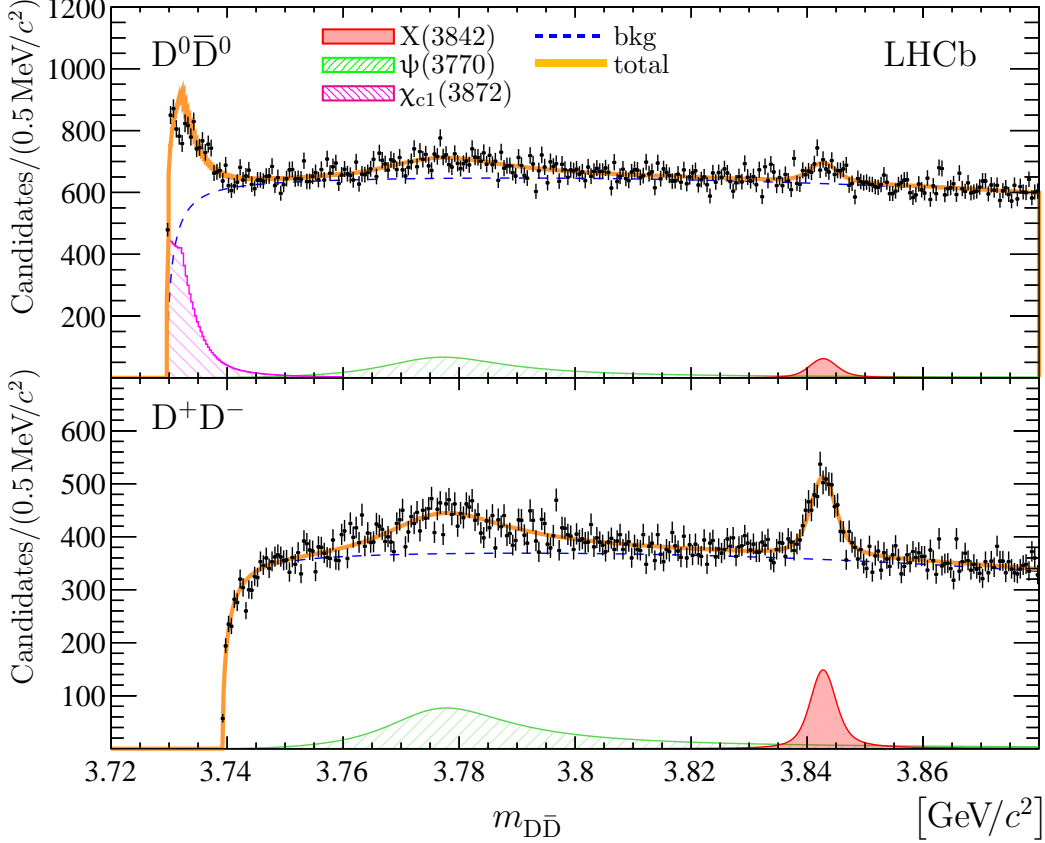


Figure 5: Mass spectra of (top) $D^0\bar{D}^0$ and (bottom) D^+D^- candidates in the near-threshold $m_{D\bar{D}} < 3.88 \text{ GeV}/c^2$ region. The result of the simultaneous fit described in the text is superimposed.

To evaluate the systematic uncertainty related to the parameterisation of the signal shape, the parameters of the relativistic Breit–Wigner functions are varied. In particular, the meson radius, entering the Blatt–Weisskopf centrifugal factor with the default value of 3.5 GeV^{-1} , is varied between 1.5 GeV^{-1} and 5 GeV^{-1} . In the case of the $X(3842)$ state, where the quantum numbers are unknown, the orbital momentum is varied between zero and four. For the $X(3842)$ and $\chi_{c2}(3930)$ states, alternative signal descriptions with multi-channel relativistic Breit–Wigner functions with $D^0\bar{D}^0$ and D^+D^- and radiative non- $D\bar{D}$ decays are used. For the $\psi(3770)$ signal, the parameters of the multi-channel relativistic P-wave Breit–Wigner function, namely the ratio of branching fractions to $D^0\bar{D}^0$ and D^+D^- final states, and the branching fraction for non- $D\bar{D}$, are varied within their known uncertainties [39].

The determination of the natural width of the $X(3842)$ and $\chi_{c2}(3930)$ states relies on accurate modelling of the detector resolution. Comparing data and simulation for decay modes with low energy release such as the $\chi_{c1} \rightarrow J/\psi \mu^+ \mu^-$ decay, agreement at the 10% level is found [46]. Even better agreement is found for b-hadron decays to pairs of open charm hadrons such as $B^0 \rightarrow D_s^+ D^-$, $\Lambda_b^0 \rightarrow \Lambda_c^+ D_s^-$ and $\Lambda_b^0 \rightarrow \Lambda_c^+ D^-$ [47], where the energy release is larger. Hence, to estimate the corresponding uncertainty the resolution scale is varied by 10% and the fit is repeated. Alternative resolution models, such as a symmetric

Table 4: Summary of systematic uncertainties for the measured masses (σ_m) and width (σ_Γ) of the X(3842), $\chi_{c2}(3930)$ and $\psi(3770)$ states. Uncertainties for the mass (width) smaller than 10 keV/ c^2 (10 keV) are not shown.

Source	X(3842)		$\chi_{c2}(3930)$		$\psi(3770)$
	σ_m [MeV/ c^2]	σ_Γ [MeV]	σ_m [MeV/ c^2]	σ_Γ [MeV]	σ_m [MeV/ c^2]
Signal model	0.02	0.02	0.01	0.15	0.62
Resolution		0.31		0.20	
Background model		0.13	0.15	0.81	0.03
Momentum scale	0.07	—	0.05	—	
D-meson masses	0.10	—	0.10	—	0.10
Sum in quadrature	0.12	0.35	0.19	0.85	0.63

double-sided Crystal Ball function [48, 49] and a symmetric variant of the Apollonios function [50] are used to estimate the uncertainty associated with this choice.

The uncertainty in the knowledge of the width of the $\psi(3770)$ resonance [39] is propagated by applying a Gaussian constraint in the fit, and it is therefore a part of the statistical uncertainty for the measured mass of the $\psi(3770)$ state. The effect of fixing the parameters of the X(3842) state in the fits in the $m_{D\bar{D}} < 3.88 \text{ GeV}/c^2$ and $m_{D\bar{D}} > 3.8 \text{ GeV}/c^2$ regions on the parameters of the $\chi_{c2}(3930)$ and $\psi(3770)$ states is found to be negligible. The effect of the poorly known shape for the $\chi_{c1}(3872) \rightarrow D^0\bar{D}^0X$ component has no visible effect on the determination of the mass of the $\psi(3770)$ state.

The impact of the choice of the background model is estimated by changing the order of the polynomial functions from second to fourth order and, for fits in the $3.80 < m_{D\bar{D}} < 3.88 \text{ GeV}/c^2$ and $m_{D\bar{D}} < 3.88 \text{ GeV}/c^2$ regions, by including an exponential factor to the background model. For the fit in the $3.80 < m_{D\bar{D}} < 3.88 \text{ GeV}/c^2$ region, the contributions from the long tails of the wide $\psi(3770)$ and $\chi_{c2}(3930)$ resonances are accounted for.

The Particle Data Group (PDG) [39] reports various heavy or exotic charmonium candidates that decay to $D\bar{D}$, $D^*\bar{D}$ and $D^*\bar{D}^*$ final states. Typically, these states are relatively broad and consequently they will only be visible as a distortion of the background shape. To study the impact of these charmonium states on the measurements made here, the decays $Z_c(3900) \rightarrow D^0D^{*-}$, $X(4020) \rightarrow D^*\bar{D}^*$, $\chi_{c0}(3860) \rightarrow D\bar{D}$, and decays of $\psi(4040)$, $\psi(4160)$, $\psi(4415)$ to $D\bar{D}$, $D^*\bar{D}$ and $D^*\bar{D}^*$ final states [39] are simulated and individually added as fit components in turn. For these studies, the measurements of the relative direct ($D\bar{D}$) and feed-down ($D^*\bar{D}$ and $D^*\bar{D}^*$) contributions [39] provide important constraints. Fits including decays of the $\chi_{c0}(3860)$, $\psi(4040)$ or $\psi(4160)$ states are found to modify the background component and cause a maximum of 0.15 MeV/ c^2 bias on the mass and a maximum of 0.5 MeV bias on the natural width of the $\chi_{c2}(3930)$ state. These are accounted for as uncertainties due to the background description. Contributions from other charmonium or charmonium-like states have no effect in the determination of the parameters of the X(3842), $\chi_{c2}(3930)$ and $\psi(3770)$ states.

An important experimental uncertainty for the mass measurements is the knowledge

of the momentum scale. This is minimised by the application of the D-mass constraints. The residual uncertainty from this source is evaluated by adjusting the momentum scale by the 3×10^{-4} uncertainty on the calibration procedure and repeating the mass fit. A further uncertainty of $0.1 \text{ MeV}/c^2$ arises from the knowledge of the D^0 and D^+ masses [39].

6 Production mechanism

The selection criteria used in this analysis significantly suppress a potential contribution from weak decays of long-lived beauty hadrons. To probe the residual contribution from b-hadron decays, the sample of $D\bar{D}$ pairs is split into two subsamples according to the value of the t_z variable [51]

$$t_z \equiv \frac{z_{D\bar{D}} - z_{PV}}{p_z} m_{D\bar{D}},$$

where $z_{D\bar{D}}$ and z_{PV} are the positions along the z -axis (the beam direction) of the reconstructed $D\bar{D}$ vertex and of the primary vertex, and p_z is the measured $D\bar{D}$ momentum in the z direction. Promptly produced charmonia are characterised by a nearly symmetric and narrow distribution around $t_z = 0$, whilst almost all $D\bar{D}$ pairs being produced in the weak decays of long-lived beauty hadrons have $t_z > 0$. Comparison of the observed yields of the $X(3842)$, $\chi_{c2}(3930)$ and $\psi(3770)$ signals for $t_z < 0$ and $t_z > 0$ subsamples shows no sizeable contributions from decays of b hadrons to the $X(3842)$ and $\chi_{c2}(3930)$ signals, while a contribution of $\sim 35\%$ to the observed yield of the $\psi(3770) \rightarrow D\bar{D}$ decays is found.

Reference [8] suggests the decay $\chi_{c2}(2^3P_2) \rightarrow \psi_3(1^3D_3)\gamma$ as a possible production mechanism for the $\psi_3(1^3D_3)$ state. The hypothesis is tested as follows. Identifying the $\chi_{c2}(3930)$ as $\chi_{c2}(2^3P_2)$ and $X(3842)$ as $\psi_3(1^3D_3)$ and taking $\Gamma(\chi_{c2}(2^3P_2) \rightarrow \psi_3(1^3D_3)\gamma)$ to be 100 keV [8], from the present measurement of the $\chi_{c2}(3930)$ state width and the observed yields of $\chi_{c2}(3930) \rightarrow D\bar{D}$ decays, at most 5% of the observed $X(3842) \rightarrow D\bar{D}$ decays can originate from the decays of the $\chi_{c2}(3930)$ state. This suggests, assuming the $\psi_3(1^3D_3)$ assignment is correct, that either $\Gamma(\chi_{c2}(2^3P_2) \rightarrow \psi_3(1^3D_3)\gamma)$ is significantly larger than expected or that a large fraction of the $X(3842)$ signal is produced via a different production mechanism.

7 Results and discussion

Using the LHCb dataset collected between 2011 and 2018, near-threshold $D\bar{D}$ mass spectra are studied and a new narrow charmonium state, the $X(3842)$, is observed in the decay modes $X(3842) \rightarrow D^0\bar{D}^0$ and $X(3842) \rightarrow D^+D^-$ with very high statistical significance. The mass and the natural width of this state are measured to be

$$\begin{aligned} m_{X(3842)} &= 3842.71 \pm 0.16 \pm 0.12 \text{ MeV}/c^2, \\ \Gamma_{X(3842)} &= 2.79 \pm 0.51 \pm 0.35 \text{ MeV}, \end{aligned}$$

where the first uncertainty is statistical and the second is systematic. The narrow natural width and measured value of the mass suggests the interpretation of the $X(3842)$ state as the $\psi_3(1^3D_3)$ charmonium state with $J^{PC} = 3^{--}$.

Table 5: Summary of mass and width measurements for the $\chi_{c2}(3930)$ state.

		$m_{\chi_{c2}(3930)}$ [MeV/ c^2]	$\Gamma_{\chi_{c2}(3930)}$ [MeV]
Belle	[17]	$3929 \pm 5 \pm 2$	$29 \pm 10 \pm 2$
BaBar	[18]	$3926.7 \pm 2.7 \pm 1.1$	$21.3 \pm 6.8 \pm 3.6$
This analysis		$3921.9 \pm 0.6 \pm 0.2$	$36.6 \pm 1.9 \pm 0.9$

Table 6: Summary of mass measurements for the $\psi(3770)$ state.

		$m_{\psi(3770)}$ [MeV/ c^2]
Shamov and Todyshev	[58]	3779.8 ± 0.6
PDG average	[39]	3778.1 ± 1.2
PDG fit	[39]	3773.13 ± 0.35
This analysis		$3778.1 \pm 0.7 \pm 0.6$

In addition, prompt hadroproduction of the $\chi_{c2}(3930)$ state is observed for the first time, and the parameters of this state are measured to be

$$\begin{aligned} m_{\chi_{c2}(3930)} &= 3921.9 \pm 0.6 \pm 0.2 \text{ MeV}/c^2, \\ \Gamma_{\chi_{c2}(3930)} &= 36.6 \pm 1.9 \pm 0.9 \text{ MeV}. \end{aligned}$$

These values are considerably more precise than previous measurements made at e^+e^- machines, as can be seen from Table 5. The mass measured in this analysis is 2σ lower than the current world average whilst the natural width is 2σ higher. It is interesting to note that the measured value of the mass is roughly midway between the masses quoted in Ref. [39] for this state and for the X(3915) meson, which is only known to decay to the $J/\psi \omega$ final state [52–56]. Further studies are needed to understand if there are two distinct charmonium states in this region or only one as suggested in Ref. [57].

Finally, prompt hadroproduction of the $\psi(3770)$ state is observed for the first time, and the mass of this state is measured to be

$$m_{\psi(3770)} = 3778.1 \pm 0.7 \pm 0.6 \text{ MeV}/c^2.$$

The measured mass agrees well with the value determined by Shamov and Todyshev [58] from available e^+e^- cross-section data. It also agrees well with and has a better precision than the current world average [39], referred as PDG average in Table 6, which is dominated by the value measured by the KEDR collaboration [42]. Reference [39] also quotes a value, referred as PDG fit, resulting from a fit that includes precision measurements of the mass difference between the $\psi(3770)$ and $\psi(2S)$ states made by the BES collaboration [43, 59, 60]. Both the measurement made here and the PDG average are in disagreement with the PDG fit value.

Acknowledgements

We express our gratitude to our colleagues in the CERN accelerator departments for the excellent performance of the LHC. We thank the technical

and administrative staff at the LHCb institutes. We acknowledge support from CERN and from the national agencies: CAPES, CNPq, FAPERJ and FINEP (Brazil); MOST and NSFC (China); CNRS/IN2P3 (France); BMBF, DFG and MPG (Germany); INFN (Italy); NWO (Netherlands); MNiSW and NCN (Poland); MEN/IFA (Romania); MSHE (Russia); MinECo (Spain); SNSF and SER (Switzerland); NASU (Ukraine); STFC (United Kingdom); NSF (USA). We acknowledge the computing resources that are provided by CERN, IN2P3 (France), KIT and DESY (Germany), INFN (Italy), SURF (Netherlands), PIC (Spain), GridPP (United Kingdom), RRCKI and Yandex LLC (Russia), CSCS (Switzerland), IFIN-HH (Romania), CBPF (Brazil), PL-GRID (Poland) and OSC (USA). We are indebted to the communities behind the multiple open-source software packages on which we depend. Individual groups or members have received support from AvH Foundation (Germany); EPLANET, Marie Skłodowska-Curie Actions and ERC (European Union); ANR, Labex P2IO and OCEVU, and Région Auvergne-Rhône-Alpes (France); Key Research Program of Frontier Sciences of CAS, CAS PIFI, and the Thousand Talents Program (China); RFBR, RSF and Yandex LLC (Russia); GVA, XuntaGal and GENCAT (Spain); the Royal Society and the Leverhulme Trust (United Kingdom); Laboratory Directed Research and Development program of LANL (USA).

References

- [1] J. J. Aubert *et al.*, *Experimental observation of a heavy particle J*, Phys. Rev. Lett. **33** (1974) 1404.
- [2] J. E. Augustin *et al.*, *Discovery of a narrow resonance in e^+e^- annihilation*, Phys. Rev. Lett. **33** (1974) 1406.
- [3] E. J. Eichten *et al.*, *Charmonium: The model*, Phys. Rev. **D17** (1978) 3090, Erratum *ibid.* **D21** (1980) 313.
- [4] Belle collaboration, S. K. Choi *et al.*, *Observation of a narrow charmonium-like state in exclusive $B^\pm \rightarrow K^\pm \pi^+ \pi^- J/\psi$* , Phys. Rev. Lett. **91** (2003) 262001, [arXiv:hep-ex/0309032](#).
- [5] E. J. Eichten, K. Lane, and C. Quigg, *B meson gateways to missing charmonium levels*, Phys. Rev. Lett. **89** (2002) 162002, [arXiv:hep-ph/0206018](#).
- [6] E. J. Eichten, K. Lane, and C. Quigg, *New states above charm threshold*, Phys. Rev. **D73** (2006) 014014, Erratum *ibid.* **D73** (2006) 079903, [arXiv:hep-ph/0511179](#).
- [7] T. Barnes and S. Godfrey, *Charmonium options for the X(3872)*, Phys. Rev. **D69** (2004) 054008, [arXiv:hep-ph/0311162](#).
- [8] T. Barnes, S. Godfrey, and E. S. Swanson, *Higher charmonia*, Phys. Rev. **D72** (2005) 054026, [arXiv:hep-ph/0505002](#).
- [9] S. F. Radford and W. W. Repko, *Potential model calculations and predictions for heavy quarkonium*, Phys. Rev. **D75** (2007) 074031, [arXiv:hep-ph/0701117](#).
- [10] S. Godfrey and N. Isgur, *Mesons in a relativized quark model with chromodynamics*, Phys. Rev. **D32** (1985) 189.
- [11] E. J. Eichten and F. Feinberg, *Spin-dependent forces in QCD*, Phys. Rev. **D23** (1981) 2724.
- [12] L. P. Fulcher, *Perturbative QCD, a universal QCD scale, long range spin orbit potential, and the properties of heavy quarkonia*, Phys. Rev. **D44** (1991) 2079.
- [13] S. N. Gupta, S. F. Radford, and W. W. Repko, *Semirelativistic potential model for heavy quarkonia*, Phys. Rev. **D34** (1986) 201.
- [14] D. Ebert, R. N. Faustov, and V. O. Galkin, *Properties of heavy quarkonia and B_c^+ mesons in the relativistic quark model*, Phys. Rev. **D67** (2003) 014027, [arXiv:hep-ph/0210381](#).
- [15] J. Zeng, J. W. Van Orden, and W. Roberts, *Heavy mesons in a relativistic model*, Phys. Rev. **D52** (1995) 5229, [arXiv:hep-ph/9412269](#).
- [16] LHCb collaboration, R. Aaij *et al.*, *Observation of a resonance in $B^+ \rightarrow K^+ \mu^+ \mu^-$ decays at low recoil*, Phys. Rev. Lett. **111** (2013) 112003, [arXiv:1307.7595](#).

- [17] Belle collaboration, S. Uehara *et al.*, *Observation of a χ_{c2} candidate in $\gamma\gamma \rightarrow D\bar{D}$ production at Belle*, Phys. Rev. Lett. **96** (2006) 082003, [arXiv:hep-ex/0512035](#).
- [18] BaBar collaboration, B. Aubert *et al.*, *Observation of the $\chi_{c2}(2P)$ meson in the reaction $\gamma\gamma \rightarrow D\bar{D}$ at BaBar*, Phys. Rev. **D81** (2010) 092003, [arXiv:1002.0281](#).
- [19] LHCb collaboration, A. A. Alves Jr. *et al.*, *The LHCb detector at the LHC*, JINST **3** (2008) S08005.
- [20] LHCb collaboration, R. Aaij *et al.*, *LHCb detector performance*, Int. J. Mod. Phys. **A30** (2015) 1530022, [arXiv:1412.6352](#).
- [21] R. Aaij *et al.*, *Performance of the LHCb Vertex Locator*, JINST **9** (2014) P09007, [arXiv:1405.7808](#).
- [22] R. Arink *et al.*, *Performance of the LHCb Outer Tracker*, JINST **9** (2014) P01002, [arXiv:1311.3893](#).
- [23] P. d'Argent *et al.*, *Improved performance of the LHCb Outer Tracker in LHC Run 2*, JINST **9** (2017) P11016, [arXiv:1708.00819](#).
- [24] LHCb collaboration, R. Aaij *et al.*, *Measurements of the Λ_b^0 , Ξ_b^- , and Ω_b^- baryon masses*, Phys. Rev. Lett. **110** (2013) 182001, [arXiv:1302.1072](#).
- [25] LHCb collaboration, R. Aaij *et al.*, *Precision measurement of D meson mass differences*, JHEP **06** (2013) 065, [arXiv:1304.6865](#).
- [26] M. Adinolfi *et al.*, *Performance of the LHCb RICH detector at the LHC*, Eur. Phys. J. **C73** (2013) 2431, [arXiv:1211.6759](#).
- [27] A. A. Alves Jr. *et al.*, *Performance of the LHCb muon system*, JINST **8** (2013) P02022, [arXiv:1211.1346](#).
- [28] R. Aaij *et al.*, *The LHCb trigger and its performance in 2011*, JINST **8** (2013) P04022, [arXiv:1211.3055](#).
- [29] T. Sjöstrand, S. Mrenna, and P. Skands, *A brief introduction to PYTHIA 8.1*, Comput. Phys. Commun. **178** (2008) 852, [arXiv:0710.3820](#); T. Sjöstrand, S. Mrenna, and P. Skands, *PYTHIA 6.4 physics and manual*, JHEP **05** (2006) 026, [arXiv:hep-ph/0603175](#).
- [30] I. Belyaev *et al.*, *Handling of the generation of primary events in GAUSS, the LHCb simulation framework*, J. Phys. Conf. Ser. **331** (2011) 032047.
- [31] D. J. Lange, *The EVTGEN particle decay simulation package*, Nucl. Instrum. Meth. **A462** (2001) 152.
- [32] P. Golonka and Z. Was, *PHOTOS Monte Carlo: A precision tool for QED corrections in Z and W decays*, Eur. Phys. J. **C45** (2006) 97, [arXiv:hep-ph/0506026](#).
- [33] Geant4 collaboration, J. Allison *et al.*, *GEANT4 developments and applications*, IEEE Trans. Nucl. Sci. **53** (2006) 270; Geant4 collaboration, S. Agostinelli *et al.*, *GEANT4: A simulation toolkit*, Nucl. Instrum. Meth. **A506** (2003) 250.

- [34] M. Clemencic *et al.*, *The LHCb simulation application, GAUSS: Design, evolution and experience*, J. Phys. Conf. Ser. **331** (2011) 032023.
- [35] LHCb collaboration, R. Aaij *et al.*, *Observation of double charm production involving open charm in pp collisions at $\sqrt{s} = 7$ TeV*, JHEP **06** (2012) 141, Addendum *ibid.* **03** (2014) 108, [arXiv:1205.0975](#).
- [36] LHCb collaboration, R. Aaij *et al.*, *Observation of associated production of a Z boson with a D meson in the forward region*, JHEP **04** (2014) 091, [arXiv:1401.3245](#).
- [37] LHCb collaboration, R. Aaij *et al.*, *Production of associated Υ and open charm hadrons in pp collisions at $\sqrt{s} = 7$ and 8 TeV via double parton scattering*, JHEP **07** (2016) 052, [arXiv:1510.05949](#).
- [38] W. D. Hulsbergen, *Decay chain fitting with a Kalman filter*, Nucl. Instrum. Meth. **A552** (2005) 566, [arXiv:physics/0503191](#).
- [39] Particle Data Group, M. Tanabashi *et al.*, *Review of particle physics*, Phys. Rev. **D98** (2018) 030001.
- [40] J. M. Blatt and V. F. Weisskopf, *Theoretical nuclear physics*, Springer, New York, 1952.
- [41] S. S. Wilks, *The large-sample distribution of the likelihood ratio for testing composite hypotheses*, Ann. Math. Stat. **9** (1938) 60.
- [42] KEDR collaboration, V. V. Anashin *et al.*, *Measurement of $\psi(3770)$ parameters*, Phys. Lett. **B711** (2012) 292, [arXiv:1109.4205](#).
- [43] BES collaboration, M. Ablikim *et al.*, *Determination of the $\psi(3770)$, $\psi(4040)$, $\psi(4160)$ and $\psi(4415)$ resonance parameters*, Phys. Lett. **B660** (2008) 315, [arXiv:0705.4500](#).
- [44] E. Braaten and M. Lu, *Line shapes of the X(3872)*, Phys. Rev. **D76** (2007) 094028, [arXiv:0709.2697](#).
- [45] E. Braaten and J. Stapleton, *Analysis of $J/\psi \pi^+ \pi^-$ and $D^0 \bar{D}^0 \pi^0$ decays of the X(3872)*, Phys. Rev. **D81** (2010) 014019, [arXiv:0907.3167](#).
- [46] LHCb collaboration, R. Aaij *et al.*, *χ_{c1} and χ_{c2} resonance parameters with the decays $\chi_{c1,c2} \rightarrow J/\psi \mu^+ \mu^-$* , Phys. Rev. Lett. **119** (2017) 221801, [arXiv:1709.04247](#).
- [47] LHCb collaboration, R. Aaij *et al.*, *Study of beauty hadron decays into pairs of charm hadrons*, Phys. Rev. Lett. **112** (2014) 202001, [arXiv:1403.3606](#).
- [48] T. Skwarnicki, *A study of the radiative cascade transitions between the Upsilon-prime and Upsilon resonances*, PhD thesis, Institute of Nuclear Physics, Krakow, 1986, DESY-F31-86-02.
- [49] LHCb collaboration, R. Aaij *et al.*, *Observation of J/ψ -pair production in pp collisions at $\sqrt{s} = 7$ TeV*, Phys. Lett. **B707** (2012) 52, [arXiv:1109.0963](#).

- [50] D. Martínez Santos and F. Dupertuis, *Mass distributions marginalized over per-event errors*, Nucl. Instrum. Meth. **A764** (2014) 150, [arXiv:1312.5000](#).
- [51] LHCb collaboration, R. Aaij *et al.*, *Measurement of J/ψ production in pp collisions at $\sqrt{s} = 7$ TeV*, Eur. Phys. J. **C71** (2011) 1645, [arXiv:1103.0423](#).
- [52] BaBar collaboration, J. P. Lees *et al.*, *Study of $X(3915) \rightarrow J/\psi \omega$ in two-photon collisions*, Phys. Rev. **D86** (2012) 072002, [arXiv:1207.2651](#).
- [53] BaBar collaboration, P. del Amo Sanchez *et al.*, *Evidence for the decay $X(3872) \rightarrow J/\psi \omega$* , Phys. Rev. **D82** (2010) 011101, [arXiv:1005.5190](#).
- [54] Belle collaboration, S. Uehara *et al.*, *Observation of a charmonium-like enhancement in the $\gamma\gamma \rightarrow J/\psi \omega$ process*, Phys. Rev. Lett. **104** (2010) 092001, [arXiv:0912.4451](#).
- [55] Belle collaboration, K. Abe *et al.*, *Observation of a near-threshold $\omega J/\psi$ mass enhancement in exclusive $B^+ \rightarrow K^+ \omega J/\psi$ decays*, Phys. Rev. Lett. **94** (2005) 182002, [arXiv:hep-ex/0408126](#).
- [56] Belle collaboration, T. Aushev *et al.*, *Study of the $B \rightarrow X(3872)(\rightarrow D^{*0} \bar{D}^0) K$ decay*, Phys. Rev. **D81** (2010) 031103, [arXiv:0810.0358](#).
- [57] Z.-Y. Zhou, Z. Xiao, and H.-Q. Zhou, *Could the $X(3915)$ and the $X(3930)$ be the same tensor state?*, Phys. Rev. Lett. **115** (2015) 022001, [arXiv:1501.00879](#).
- [58] A. G. Shamov and K. Yu. Todyshev, *Analysis of BaBar, Belle, BES-II, CLEO and KEDR data on $\psi(3770)$ line shape and determination of the resonance parameters*, Phys. Lett. **B769** (2017) 187, [arXiv:1610.02147](#).
- [59] BES collaboration, M. Ablikim *et al.*, *Precision measurements of the mass, the widths of $\psi(3770)$ resonance and the cross section $\sigma(e^+e^- \rightarrow \psi(3770))$ at $E_{\text{cm}} = 3.7724$ GeV*, Phys. Lett. **B652** (2007) 238, [arXiv:hep-ex/0612056](#).
- [60] BES collaboration, M. Ablikim *et al.*, *Measurements of the branching fractions for $\psi(3770) \rightarrow D^0 \bar{D}^0, D^+ D^-$, $D \bar{D}$ and the resonance parameters of $\psi(3770)$ and $\psi(2S)$* , Phys. Rev. Lett. **97** (2006) 121801, [arXiv:hep-ex/0605107](#).

LHCb Collaboration

R. Aaij²⁹, C. Abellán Beteta⁴⁶, B. Adeva⁴³, M. Adinolfi⁵⁰, C.A. Aidala⁷⁷, Z. Ajaltouni⁷, S. Akar⁶¹, P. Albicocco²⁰, J. Albrecht¹², F. Alessio⁴⁴, M. Alexander⁵⁵, A. Alfonso Alberó⁴², G. Alkhazov⁴¹, P. Alvarez Cartelle⁵⁷, A.A. Alves Jr⁴³, S. Amato², Y. Amhis⁹, L. An¹⁹, L. Anderlini¹⁹, G. Andreassi⁴⁵, M. Andreotti¹⁸, J.E. Andrews⁶², F. Archilli²⁹, J. Arnau Romeu⁸, A. Artamonov⁴⁰, M. Artuso⁶³, K. Arzymatov³⁸, E. Aslanides⁸, M. Atzeni⁴⁶, B. Audurier²⁴, S. Bachmann¹⁴, J.J. Back⁵², S. Baker⁵⁷, V. Balagura^{9,b}, W. Baldini^{18,44}, A. Baranov³⁸, R.J. Barlow⁵⁸, S. Barsuk⁹, W. Barter⁵⁷, M. Bartolini²¹, F. Baryshnikov⁷³, V. Batozskaya³³, B. Batsukh⁶³, A. Battig¹², V. Battista⁴⁵, A. Bay⁴⁵, F. Bedeschi²⁶, I. Bediaga¹, A. Beiter⁶³, L.J. Bei²⁹, S. Belin²⁴, N. Bely⁴, V. Bellec⁴⁵, N. Belloli^{22,i}, K. Belous⁴⁰, I. Belyaev³⁵, G. Bencivenni²⁰, E. Ben-Haim¹⁰, S. Benson²⁹, S. Beranek¹¹, A. Berezhnoy³⁶, R. Bernet⁴⁶, D. Berninghoff¹⁴, E. Bertholet¹⁰, A. Bertolin²⁵, C. Betancourt⁴⁶, F. Betti^{17,e}, M.O. Bettler⁵¹, Ia. Bezshyiko⁴⁶, S. Bhasin⁵⁰, J. Bhom³¹, M.S. Bieker¹², S. Bifani⁴⁹, P. Billoir¹⁰, A. Birnkraut¹², A. Bizzeti^{19,u}, M. Bjørn⁵⁹, M.P. Blago⁴⁴, T. Blake⁵², F. Blanc⁴⁵, S. Blusk⁶³, D. Bobulska⁵⁵, V. Bocci²⁸, O. Boente Garcia⁴³, T. Boettcher⁶⁰, A. Bondar^{39,x}, N. Bondar⁴¹, S. Borghi^{58,44}, M. Borisyak³⁸, M. Borsato¹⁴, M. Boubdir¹¹, T.J.V. Bowcock⁵⁶, C. Bozzi^{18,44}, S. Braun¹⁴, M. Brodski⁴⁴, J. Brodzicka³¹, A. Brossa Gonzalo⁵², D. Brundu^{24,44}, E. Buchanan⁵⁰, A. Buonaura⁴⁶, C. Buri⁵⁸, A. Bursche²⁴, J. Buytaert⁴⁴, W. Byczynski⁴⁴, S. Cadceddu²⁴, H. Cai⁶⁷, R. Calabrese^{18,g}, S. Cali²⁰, R. Calladine⁴⁹, M. Calvi^{22,i}, M. Calvo Gomez^{42,m}, A. Camboni^{42,m}, P. Campana²⁰, D.H. Campora Perez⁴⁴, L. Capriotti^{17,e}, A. Carbone^{17,e}, G. Carboni²⁷, R. Cardinale²¹, A. Cardini²⁴, P. Carniti^{22,i}, K. Carvalho Akiba², G. Casse⁵⁶, M. Cattaneo⁴⁴, G. Cavallero²¹, R. Cenci^{26,p}, M.G. Chapman⁵⁰, M. Charles^{10,44}, Ph. Charpentier⁴⁴, G. Chatzikonstantinidis⁴⁹, M. Chefdeville⁶, V. Chekalina³⁸, C. Chen³, S. Chen²⁴, S.-G. Chitic⁴⁴, V. Chobanova⁴³, M. Chruszcz⁴⁴, A. Chubykin⁴¹, P. Ciambone²⁰, X. Cid Vidal⁴³, G. Ciezarek⁴⁴, F. Cindolo¹⁷, P.E.L. Clarke⁵⁴, M. Clemencic⁴⁴, H.V. Cliff⁵¹, J. Closier⁴⁴, V. Coco⁴⁴, J.A.B. Coelho⁹, J. Cogan⁸, E. Cogneras⁷, L. Cojocariu³⁴, P. Collins⁴⁴, T. Colombo⁴⁴, A. Comerma-Montells¹⁴, A. Contu²⁴, G. Coombs⁴⁴, S. Coquereau⁴², G. Corti⁴⁴, C.M. Costa Sobral⁵², B. Couturier⁴⁴, G.A. Cowan⁵⁴, D.C. Craik⁶⁰, A. Crocombe⁵², M. Cruz Torres¹, R. Currie⁵⁴, C.L. Da Silva⁷⁸, E. Dall'Occo²⁹, J. Dalseno^{43,v}, C. D'Ambrosio⁴⁴, A. Danilina³⁵, P. d'Argent¹⁴, A. Davis⁵⁸, O. De Aguiar Francisco⁴⁴, K. De Bruyn⁴⁴, S. De Capua⁵⁸, M. De Cian⁴⁵, J.M. De Miranda¹, L. De Paula², M. De Serio^{16,d}, P. De Simone²⁰, J.A. de Vries²⁹, C.T. Dean⁵⁵, W. Dean⁷⁷, D. Decamp⁶, L. Del Buono¹⁰, B. Delaney⁵¹, H.-P. Dembinski¹³, M. Demmer¹², A. Dendek³², D. Derkach⁷⁴, O. Deschamps⁷, F. Desse⁹, F. Dettori²⁴, B. Dey⁶⁸, A. Di Canto⁴⁴, P. Di Nezza²⁰, S. Didenko⁷³, H. Dijkstra⁴⁴, F. Dordei²⁴, M. Dorigo^{26,y}, A.C. dos Reis¹, A. Dosil Suárez⁴³, L. Douglas⁵⁵, A. Dovbnya⁴⁷, K. Dreimanis⁵⁶, L. Dufour⁴⁴, G. Dujany¹⁰, P. Durante⁴⁴, J.M. Durham⁷⁸, D. Dutta⁵⁸, R. Dzhelyadin^{40,†}, M. Dziwiewiecki¹⁴, A. Dziurda³¹, A. Dzyuba⁴¹, S. Easo⁵³, U. Egede⁵⁷, V. Egorychev³⁵, S. Eidelman^{39,x}, S. Eisenhardt⁵⁴, U. Eitschberger¹², R. Ekelhof¹², L. Eklund⁵⁵, S. Ely⁶³, A. Ene³⁴, S. Escher¹¹, S. Esen²⁹, T. Evans⁶¹, A. Falabella¹⁷, C. Färber⁴⁴, N. Farley⁴⁹, S. Farry⁵⁶, D. Fazzini^{22,i}, M. Féo⁴⁴, P. Fernandez Declara⁴⁴, A. Fernandez Prieto⁴³, F. Ferrari^{17,e}, L. Ferreira Lopes⁴⁵, F. Ferreira Rodrigues², S. Ferreres Sole²⁹, M. Ferro-Luzzi⁴⁴, S. Filippov³⁷, R.A. Fini¹⁶, M. Fiorini^{18,g}, M. Firlej³², C. Fitzpatrick⁴⁴, T. Fiutowski³², F. Fleuret^{9,b}, M. Fontana⁴⁴, F. Fontanelli^{21,h}, R. Forty⁴⁴, V. Franco Lima⁵⁶, M. Frank⁴⁴, C. Frei⁴⁴, J. Fu^{23,q}, W. Funk⁴⁴, E. Gabriel⁵⁴, A. Gallas Torreira⁴³, D. Galli^{17,e}, S. Gallorini²⁵, S. Gambetta⁵⁴, Y. Gan³, M. Gandelman², P. Gandini²³, Y. Gao³, L.M. Garcia Martin⁷⁶, J. García Pardiñas⁴⁶, B. Garcia Plana⁴³, J. Garra Tico⁵¹, L. Garrido⁴², D. Gascon⁴², C. Gaspar⁴⁴, G. Gazzoni⁷, D. Gerick¹⁴, E. Gersabeck⁵⁸, M. Gersabeck⁵⁸, T. Gershon⁵², D. Gerstel⁸, Ph. Ghez⁶, V. Gibson⁵¹, O.G. Girard⁴⁵, P. Gironella Gironell⁴², L. Giubega³⁴, K. Gizdov⁵⁴, V.V. Gligorov¹⁰, C. Göbel⁶⁵, D. Golubkov³⁵, A. Golutvin^{57,73}, A. Gomes^{1,a},

I.V. Gorelov³⁶, C. Gotti^{22,i}, E. Govorkova²⁹, J.P. Grabowski¹⁴, R. Graciani Diaz⁴²,
 L.A. Granado Cardoso⁴⁴, E. Graugés⁴², E. Graverini⁴⁶, G. Graziani¹⁹, A. Grecu³⁴, R. Greim²⁹,
 P. Griffith²⁴, L. Grillo⁵⁸, L. Gruber⁴⁴, B.R. Gruberg Cazon⁵⁹, C. Gu³, E. Gushchin³⁷,
 A. Guth¹¹, Yu. Guz^{40,44}, T. Gys⁴⁴, T. Hadavizadeh⁵⁹, C. Hadjivasiliou⁷, G. Haefeli⁴⁵, C. Haen⁴⁴,
 S.C. Haines⁵¹, B. Hamilton⁶², Q. Han⁶⁸, X. Han¹⁴, T.H. Hancock⁵⁹, S. Hansmann-Menzemer¹⁴,
 N. Harnew⁵⁹, T. Harrison⁵⁶, C. Hasse⁴⁴, M. Hatch⁴⁴, J. He⁴, M. Hecker⁵⁷, K. Heinicke¹²,
 A. Heister¹², K. Hennessy⁵⁶, L. Henry⁷⁶, M. Heß⁷⁰, J. Heuel¹¹, A. Hicheur⁶⁴,
 R. Hidalgo Charman⁵⁸, D. Hill⁵⁹, M. Hilton⁵⁸, P.H. Hopchev⁴⁵, J. Hu¹⁴, W. Hu⁶⁸, W. Huang⁴,
 Z.C. Huard⁶¹, W. Hulsbergen²⁹, T. Humair⁵⁷, M. Hushchyn⁷⁴, D. Hutchcroft⁵⁶, D. Hynds²⁹,
 P. Ibis¹², M. Idzik³², P. Ilten⁴⁹, A. Inglessi⁴¹, A. Inyakin⁴⁰, K. Ivshin⁴¹, R. Jacobsson⁴⁴,
 S. Jakobsen⁴⁴, J. Jalocha⁵⁹, E. Jans²⁹, B.K. Jashal⁷⁶, A. Jawahery⁶², F. Jiang³, M. John⁵⁹,
 D. Johnson⁴⁴, C.R. Jones⁵¹, C. Joram⁴⁴, B. Jost⁴⁴, N. Jurik⁵⁹, S. Kandybei⁴⁷, M. Karacson⁴⁴,
 J.M. Kariuki⁵⁰, S. Karodia⁵⁵, N. Kazeev⁷⁴, M. Kecke¹⁴, F. Keizer⁵¹, M. Kelsey⁶³, M. Kenzie⁵¹,
 T. Ketel³⁰, B. Khanji⁴⁴, A. Kharisova⁷⁵, C. Khurewathanakul⁴⁵, K.E. Kim⁶³, T. Kirn¹¹,
 V.S. Kirsbaum⁴⁵, S. Klaver²⁰, K. Klimaszewski³³, S. Koliiev⁴⁸, M. Kolpin¹⁴, R. Kopečna¹⁴,
 P. Koppenburg²⁹, I. Kostiuik^{29,48}, S. Kotriakhova⁴¹, M. Kozeiha⁷, L. Kravchuk³⁷, M. Kreps⁵²,
 F. Kress⁵⁷, S. Kretzschmar¹¹, P. Krokovny^{39,x}, W. Krupa³², W. Krzemien³³, W. Kucewicz^{31,l},
 M. Kucharczyk³¹, V. Kudryavtsev^{39,x}, G.J. Kunde⁷⁸, A.K. Kuonen⁴⁵, T. Kvaratskheliya³⁵,
 D. Lacarrere⁴⁴, G. Lafferty⁵⁸, A. Lai²⁴, D. Lancierini⁴⁶, G. Lanfranchi²⁰, C. Langenbruch¹¹,
 T. Latham⁵², C. Lazzeroni⁴⁹, R. Le Gac⁸, R. Lefèvre⁷, A. Leflat³⁶, F. Lemaitre⁴⁴, O. Leroy⁸,
 T. Lesiak³¹, B. Leverington¹⁴, H. Li⁶⁶, P.-R. Li^{4,ab}, X. Li⁷⁸, Y. Li⁵, Z. Li⁶³, X. Liang⁶³,
 T. Likhomanenko⁷², R. Lindner⁴⁴, F. Lionetto⁴⁶, V. Lisovskyi⁹, G. Liu⁶⁶, X. Liu³, D. Loh⁵²,
 A. Loi²⁴, I. Longstaff⁵⁵, J.H. Lopes², G. Loustau⁴⁶, G.H. Lovell⁵¹, D. Lucchesi^{25,o},
 M. Lucio Martinez⁴³, Y. Luo³, A. Lupato²⁵, E. Luppi^{18,g}, O. Lupton⁵², A. Lusiani²⁶, X. Lyu⁴,
 F. Machefert⁹, F. Maciuc³⁴, V. Macko⁴⁵, P. Mackowiak¹², S. Maddrell-Mander⁵⁰, O. Maev^{41,44},
 K. Maguire⁵⁸, D. Maisuzenko⁴¹, M.W. Majewski³², S. Malde⁵⁹, B. Malecki⁴⁴, A. Malinin⁷²,
 T. Maltsev^{39,x}, H. Malygina¹⁴, G. Manca^{24,f}, G. Mancinelli⁸, D. Marangotto^{23,q}, J. Maratas^{7,w},
 J.F. Marchand⁶, U. Marconi¹⁷, C. Marin Benito⁹, M. Marinangeli⁴⁵, P. Marino⁴⁵, J. Marks¹⁴,
 P.J. Marshall⁵⁶, G. Martellotti²⁸, M. Martinelli^{44,22}, D. Martinez Santos⁴³, F. Martinez Vidal⁷⁶,
 A. Massafferri¹, M. Materok¹¹, R. Matev⁴⁴, A. Mathad⁴⁶, Z. Mathe⁴⁴, V. Matiunin³⁵,
 C. Matteuzzi²², K.R. Mattioli⁷⁷, A. Mauri⁴⁶, E. Maurice^{9,b}, B. Maurin⁴⁵, M. McCann^{57,44},
 A. McNab⁵⁸, R. McNulty¹⁵, J.V. Mead⁵⁶, B. Meadows⁶¹, C. Meaux⁸, N. Meinert⁷⁰,
 D. Melnychuk³³, M. Merk²⁹, A. Merli^{23,q}, E. Michielin²⁵, D.A. Milanese⁶⁹, E. Millard⁵²,
 M.-N. Minard⁶, L. Minzoni^{18,g}, D.S. Mitzel¹⁴, A. Mödden¹², A. Mogini¹⁰, R.D. Moise⁵⁷,
 T. Mombächer¹², I.A. Monroy⁶⁹, S. Monteil⁷, M. Morandin²⁵, G. Morello²⁰, M.J. Morello^{26,t},
 J. Moron³², A.B. Morris⁸, R. Mountain⁶³, F. Muheim⁵⁴, M. Mukherjee⁶⁸, M. Mulder²⁹,
 D. Müller⁴⁴, J. Müller¹², K. Müller⁴⁶, V. Müller¹², C.H. Murphy⁵⁹, D. Murray⁵⁸, P. Naik⁵⁰,
 T. Nakada⁴⁵, R. Nandakumar⁵³, A. Nandi⁵⁹, T. Nanut⁴⁵, I. Nasteva², M. Needham⁵⁴,
 N. Neri^{23,q}, S. Neubert¹⁴, N. Neufeld⁴⁴, R. Newcombe⁵⁷, T.D. Nguyen⁴⁵, C. Nguyen-Mau^{45,n},
 S. Nieswand¹¹, R. Niet¹², N. Nikitin³⁶, N.S. Nolte⁴⁴, A. Oblakowska-Mucha³², V. Obraztsov⁴⁰,
 S. Ogilvy⁵⁵, D.P. O'Hanlon¹⁷, R. Oldeman^{24,f}, C.J.G. Onderwater⁷¹, J. D. Osborn⁷⁷,
 A. Ossowska³¹, J.M. Otalora Goicochea², T. Ovsiannikova³⁵, P. Owen⁴⁶, A. Oyangueren⁷⁶,
 P.R. Pais⁴⁵, T. Pajero^{26,t}, A. Palano¹⁶, M. Palutan²⁰, G. Panshin⁷⁵, A. Papanestis⁵³,
 M. Pappagallo⁵⁴, L.L. Pappalardo^{18,g}, W. Parker⁶², C. Parkes^{58,44}, G. Passaleva^{19,44},
 A. Pastore¹⁶, M. Patel⁵⁷, C. Patrignani^{17,e}, A. Pearce⁴⁴, A. Pellegrino²⁹, G. Penso²⁸,
 M. Pepe Altarelli⁴⁴, S. Perazzini¹⁷, D. Pereima³⁵, P. Perret⁷, L. Pescatore⁴⁵, K. Petridis⁵⁰,
 A. Petrolini^{21,h}, A. Petrov⁷², S. Petrucci⁵⁴, M. Petruzzo^{23,q}, B. Pietrzyk⁶, G. Pietrzyk⁴⁵,
 M. Pikies³¹, M. Pili⁵⁹, D. Pinci²⁸, J. Pinzino⁴⁴, F. Pisani⁴⁴, A. Piucci¹⁴, V. Placinta³⁴,
 S. Playfer⁵⁴, J. Plews⁴⁹, M. Plo Casasus⁴³, F. Polci¹⁰, M. Poli Lener²⁰, M. Poliakov⁶³,
 A. Poluektov⁸, N. Polukhina^{73,c}, I. Polyakov⁶³, E. Polycarpo², G.J. Pomery⁵⁰, S. Ponce⁴⁴,

A. Popov⁴⁰, D. Popov^{49,13}, S. Poslavskii⁴⁰, E. Price⁵⁰, C. Prouve⁴³, V. Pugatch⁴⁸,
 A. Puig Navarro⁴⁶, H. Pullen⁵⁹, G. Punzi^{26,p}, W. Qian⁴, J. Qin⁴, R. Quagliani¹⁰, B. Quintana⁷,
 N.V. Raab¹⁵, B. Rachwal³², J.H. Rademacker⁵⁰, M. Rama²⁶, M. Ramos Pernas⁴³, M.S. Rangel²,
 F. Ratnikov^{38,74}, G. Raven³⁰, M. Ravonel Salzgeber⁴⁴, M. Reboud⁶, F. Redi⁴⁵, S. Reichert¹²,
 F. Reiss¹⁰, C. Remon Alepuz⁷⁶, Z. Ren³, V. Renaudin⁵⁹, S. Ricciardi⁵³, S. Richards⁵⁰,
 K. Rinnert⁵⁶, P. Robbe⁹, A. Robert¹⁰, A.B. Rodrigues⁴⁵, E. Rodrigues⁶¹,
 J.A. Rodriguez Lopez⁶⁹, M. Roehrken⁴⁴, S. Roiser⁴⁴, A. Rollings⁵⁹, V. Romanovskiy⁴⁰,
 A. Romero Vidal⁴³, J.D. Roth⁷⁷, M. Rotondo²⁰, M.S. Rudolph⁶³, T. Ruf⁴⁴, J. Ruiz Vidal⁷⁶,
 J.J. Saborido Silva⁴³, N. Sagidova⁴¹, B. Saitta^{24,f}, V. Salustino Guimaraes⁶⁵, C. Sanchez Gras²⁹,
 C. Sanchez Mayordomo⁷⁶, B. Sanmartin Sedes⁴³, R. Santacesaria²⁸, C. Santamarina Rios⁴³,
 M. Santimaria^{20,44}, E. Santovetti^{27,j}, G. Sarpis⁵⁸, A. Sarti^{20,k}, C. Satriano^{28,s}, A. Satta²⁷,
 M. Saur⁴, D. Savrina^{35,36}, S. Schael¹¹, M. Schellenberg¹², M. Schiller⁵⁵, H. Schindler⁴⁴,
 M. Schmelling¹³, T. Schmelzer¹², B. Schmidt⁴⁴, O. Schneider⁴⁵, A. Schopper⁴⁴, H.F. Schreiner⁶¹,
 M. Schubiger⁴⁵, S. Schulte⁴⁵, M.H. Schune⁹, R. Schwemmer⁴⁴, B. Sciascia²⁰, A. Sciubba^{28,k},
 A. Semennikov³⁵, E.S. Sepulveda¹⁰, A. Sergi^{49,44}, N. Serra⁴⁶, J. Serrano⁸, L. Sestini²⁵,
 A. Seuthe¹², P. Seyfert⁴⁴, M. Shapkin⁴⁰, T. Shears⁵⁶, L. Shekhtman^{39,x}, V. Shevchenko⁷²,
 E. Shmanin⁷³, B.G. Siddi¹⁸, R. Silva Coutinho⁴⁶, L. Silva de Oliveira², G. Simi^{25,o},
 S. Simone^{16,d}, I. Skiba¹⁸, N. Skidmore¹⁴, T. Skwarnicki⁶³, M.W. Slater⁴⁹, J.G. Smeaton⁵¹,
 E. Smith¹¹, I.T. Smith⁵⁴, M. Smith⁵⁷, M. Soares¹⁷, I. Soares Lavra¹, M.D. Sokoloff⁶¹,
 F.J.P. Soler⁵⁵, B. Souza De Paula², B. Spaan¹², E. Spadaro Norella^{23,q}, P. Spradlin⁵⁵,
 F. Stagni⁴⁴, M. Stahl¹⁴, S. Stahl⁴⁴, P. Stefko⁴⁵, S. Stefkova⁵⁷, O. Steinkamp⁴⁶, S. Stemmler¹⁴,
 O. Stenyakin⁴⁰, M. Stepanova⁴¹, H. Stevens¹², A. Stocchi⁹, S. Stone⁶³, S. Stracka²⁶,
 M.E. Stramaglia⁴⁵, M. Straticiu³⁴, U. Straumann⁴⁶, S. Strokov⁷⁵, J. Sun³, L. Sun⁶⁷, Y. Sun⁶²,
 K. Swientek³², A. Szabelski³³, T. Szumlak³², M. Szymanski⁴, Z. Tang³, T. Tekampe¹²,
 G. Tellarini¹⁸, F. Teubert⁴⁴, E. Thomas⁴⁴, M.J. Tilley⁵⁷, V. Tisserand⁷, S. T'Jampens⁶,
 M. Tobin⁵, S. Tolk⁴⁴, L. Tomassetti^{18,g}, D. Tonelli²⁶, D.Y. Tou¹⁰, R. Tourinho Jadallah Aoude¹,
 E. Tournefier⁶, M. Traill⁵⁵, M.T. Tran⁴⁵, A. Trisovic⁵¹, A. Tsaregorodtsev⁸, G. Tuci^{26,44,p},
 A. Tully⁵¹, N. Tuning²⁹, A. Ukleja³³, A. Usachov⁹, A. Ustyuzhanin^{38,74}, U. Uwer¹⁴,
 A. Vagner⁷⁵, V. Vagnoni¹⁷, A. Valassi⁴⁴, S. Valat⁴⁴, G. Valenti¹⁷, M. van Beuzekom²⁹,
 H. Van Hecke⁷⁸, E. van Herwijnen⁴⁴, C.B. Van Hulse¹⁵, J. van Tilburg²⁹, M. van Veghel²⁹,
 A. Vasiliev⁴⁰, R. Vazquez Gomez⁴⁴, P. Vazquez Regueiro⁴³, C. Vázquez Sierra²⁹, S. Vecchi¹⁸,
 J.J. Velthuis⁵⁰, M. Veltri^{19,r}, A. Venkateswaran⁶³, M. Vernet⁷, M. Veronesi²⁹, M. Vesterinen⁵²,
 J.V. Viana Barbosa⁴⁴, D. Vieira⁴, M. Vieites Diaz⁴³, H. Viemann⁷⁰, X. Vilasis-Cardona^{42,m},
 A. Vitkovskiy²⁹, M. Vitti⁵¹, V. Volkov³⁶, A. Vollhardt⁴⁶, D. Vom Bruch¹⁰, B. Voneki⁴⁴,
 A. Vorobyev⁴¹, V. Vorobyev^{39,x}, N. Voropaev⁴¹, R. Waldi⁷⁰, J. Walsh²⁶, J. Wang⁵, M. Wang³,
 Y. Wang⁶⁸, Z. Wang⁴⁶, D.R. Ward⁵¹, H.M. Wark⁵⁶, N.K. Watson⁴⁹, D. Websdale⁵⁷,
 A. Weiden⁴⁶, C. Weisser⁶⁰, M. Whitehead¹¹, G. Wilkinson⁵⁹, M. Wilkinson⁶³, I. Williams⁵¹,
 M. Williams⁶⁰, M.R.J. Williams⁵⁸, T. Williams⁴⁹, F.F. Wilson⁵³, M. Winn⁹, W. Wislicki³³,
 M. Witek³¹, G. Wormser⁹, S.A. Wotton⁵¹, K. Wyllie⁴⁴, D. Xiao⁶⁸, Y. Xie⁶⁸, H. Xing⁶⁶, A. Xu³,
 M. Xu⁶⁸, Q. Xu⁴, Z. Xu⁶, Z. Xu³, Z. Yang³, Z. Yang⁶², Y. Yao⁶³, L.E. Yeomans⁵⁶, H. Yin⁶⁸,
 J. Yu^{68,aa}, X. Yuan⁶³, O. Yushchenko⁴⁰, K.A. Zarebski⁴⁹, M. Zavertyaev^{13,c}, M. Zeng³,
 D. Zhang⁶⁸, L. Zhang³, W.C. Zhang^{3,z}, Y. Zhang⁴⁴, A. Zhelezov¹⁴, Y. Zheng⁴, X. Zhu³,
 V. Zhukov^{11,36}, J.B. Zonneveld⁵⁴, S. Zucchelli^{17,e}.

¹Centro Brasileiro de Pesquisas Físicas (CBPF), Rio de Janeiro, Brazil

²Universidade Federal do Rio de Janeiro (UFRJ), Rio de Janeiro, Brazil

³Center for High Energy Physics, Tsinghua University, Beijing, China

⁴University of Chinese Academy of Sciences, Beijing, China

⁵Institute Of High Energy Physics (ihep), Beijing, China

⁶Univ. Grenoble Alpes, Univ. Savoie Mont Blanc, CNRS, IN2P3-LAPP, Annecy, France

⁷Université Clermont Auvergne, CNRS/IN2P3, LPC, Clermont-Ferrand, France

- ⁸ Aix Marseille Univ, CNRS/IN2P3, CPPM, Marseille, France
- ⁹ LAL, Univ. Paris-Sud, CNRS/IN2P3, Université Paris-Saclay, Orsay, France
- ¹⁰ LPNHE, Sorbonne Université, Paris Diderot Sorbonne Paris Cité, CNRS/IN2P3, Paris, France
- ¹¹ I. Physikalisches Institut, RWTH Aachen University, Aachen, Germany
- ¹² Fakultät Physik, Technische Universität Dortmund, Dortmund, Germany
- ¹³ Max-Planck-Institut für Kernphysik (MPIK), Heidelberg, Germany
- ¹⁴ Physikalisches Institut, Ruprecht-Karls-Universität Heidelberg, Heidelberg, Germany
- ¹⁵ School of Physics, University College Dublin, Dublin, Ireland
- ¹⁶ INFN Sezione di Bari, Bari, Italy
- ¹⁷ INFN Sezione di Bologna, Bologna, Italy
- ¹⁸ INFN Sezione di Ferrara, Ferrara, Italy
- ¹⁹ INFN Sezione di Firenze, Firenze, Italy
- ²⁰ INFN Laboratori Nazionali di Frascati, Frascati, Italy
- ²¹ INFN Sezione di Genova, Genova, Italy
- ²² INFN Sezione di Milano-Bicocca, Milano, Italy
- ²³ INFN Sezione di Milano, Milano, Italy
- ²⁴ INFN Sezione di Cagliari, Monserrato, Italy
- ²⁵ INFN Sezione di Padova, Padova, Italy
- ²⁶ INFN Sezione di Pisa, Pisa, Italy
- ²⁷ INFN Sezione di Roma Tor Vergata, Roma, Italy
- ²⁸ INFN Sezione di Roma La Sapienza, Roma, Italy
- ²⁹ Nikhef National Institute for Subatomic Physics, Amsterdam, Netherlands
- ³⁰ Nikhef National Institute for Subatomic Physics and VU University Amsterdam, Amsterdam, Netherlands
- ³¹ Henryk Niewodniczanski Institute of Nuclear Physics Polish Academy of Sciences, Kraków, Poland
- ³² AGH - University of Science and Technology, Faculty of Physics and Applied Computer Science, Kraków, Poland
- ³³ National Center for Nuclear Research (NCBJ), Warsaw, Poland
- ³⁴ Horia Hulubei National Institute of Physics and Nuclear Engineering, Bucharest-Magurele, Romania
- ³⁵ Institute of Theoretical and Experimental Physics NRC Kurchatov Institute (ITEP NRC KI), Moscow, Russia, Moscow, Russia
- ³⁶ Institute of Nuclear Physics, Moscow State University (SINP MSU), Moscow, Russia
- ³⁷ Institute for Nuclear Research of the Russian Academy of Sciences (INR RAS), Moscow, Russia
- ³⁸ Yandex School of Data Analysis, Moscow, Russia
- ³⁹ Budker Institute of Nuclear Physics (SB RAS), Novosibirsk, Russia
- ⁴⁰ Institute for High Energy Physics NRC Kurchatov Institute (IHEP NRC KI), Protvino, Russia, Protvino, Russia
- ⁴¹ Petersburg Nuclear Physics Institute NRC Kurchatov Institute (PNPI NRC KI), Gatchina, Russia, St.Petersburg, Russia
- ⁴² ICCUB, Universitat de Barcelona, Barcelona, Spain
- ⁴³ Instituto Galego de Física de Altas Enerxías (IGFAE), Universidade de Santiago de Compostela, Santiago de Compostela, Spain
- ⁴⁴ European Organization for Nuclear Research (CERN), Geneva, Switzerland
- ⁴⁵ Institute of Physics, Ecole Polytechnique Fédérale de Lausanne (EPFL), Lausanne, Switzerland
- ⁴⁶ Physik-Institut, Universität Zürich, Zürich, Switzerland
- ⁴⁷ NSC Kharkiv Institute of Physics and Technology (NSC KIPT), Kharkiv, Ukraine
- ⁴⁸ Institute for Nuclear Research of the National Academy of Sciences (KINR), Kyiv, Ukraine
- ⁴⁹ University of Birmingham, Birmingham, United Kingdom
- ⁵⁰ H.H. Wills Physics Laboratory, University of Bristol, Bristol, United Kingdom
- ⁵¹ Cavendish Laboratory, University of Cambridge, Cambridge, United Kingdom
- ⁵² Department of Physics, University of Warwick, Coventry, United Kingdom
- ⁵³ STFC Rutherford Appleton Laboratory, Didcot, United Kingdom
- ⁵⁴ School of Physics and Astronomy, University of Edinburgh, Edinburgh, United Kingdom
- ⁵⁵ School of Physics and Astronomy, University of Glasgow, Glasgow, United Kingdom
- ⁵⁶ Oliver Lodge Laboratory, University of Liverpool, Liverpool, United Kingdom
- ⁵⁷ Imperial College London, London, United Kingdom

- ⁵⁸*School of Physics and Astronomy, University of Manchester, Manchester, United Kingdom*
⁵⁹*Department of Physics, University of Oxford, Oxford, United Kingdom*
⁶⁰*Massachusetts Institute of Technology, Cambridge, MA, United States*
⁶¹*University of Cincinnati, Cincinnati, OH, United States*
⁶²*University of Maryland, College Park, MD, United States*
⁶³*Syracuse University, Syracuse, NY, United States*
⁶⁴*Laboratory of Mathematical and Subatomic Physics , Constantine, Algeria, associated to ²*
⁶⁵*Pontifícia Universidade Católica do Rio de Janeiro (PUC-Rio), Rio de Janeiro, Brazil, associated to ²*
⁶⁶*South China Normal University, Guangzhou, China, associated to ³*
⁶⁷*School of Physics and Technology, Wuhan University, Wuhan, China, associated to ³*
⁶⁸*Institute of Particle Physics, Central China Normal University, Wuhan, Hubei, China, associated to ³*
⁶⁹*Departamento de Física , Universidad Nacional de Colombia, Bogota, Colombia, associated to ¹⁰*
⁷⁰*Institut für Physik, Universität Rostock, Rostock, Germany, associated to ¹⁴*
⁷¹*Van Swinderen Institute, University of Groningen, Groningen, Netherlands, associated to ²⁹*
⁷²*National Research Centre Kurchatov Institute, Moscow, Russia, associated to ³⁵*
⁷³*National University of Science and Technology “MISIS”, Moscow, Russia, associated to ³⁵*
⁷⁴*National Research University Higher School of Economics, Moscow, Russia, associated to ³⁸*
⁷⁵*National Research Tomsk Polytechnic University, Tomsk, Russia, associated to ³⁵*
⁷⁶*Instituto de Física Corpuscular, Centro Mixto Universidad de Valencia - CSIC, Valencia, Spain, associated to ⁴²*
⁷⁷*University of Michigan, Ann Arbor, United States, associated to ⁶³*
⁷⁸*Los Alamos National Laboratory (LANL), Los Alamos, United States, associated to ⁶³*

^a*Universidade Federal do Triângulo Mineiro (UFMT), Uberaba-MG, Brazil*

^b*Laboratoire Leprince-Ringuet, Palaiseau, France*

^c*P.N. Lebedev Physical Institute, Russian Academy of Science (LPI RAS), Moscow, Russia*

^d*Università di Bari, Bari, Italy*

^e*Università di Bologna, Bologna, Italy*

^f*Università di Cagliari, Cagliari, Italy*

^g*Università di Ferrara, Ferrara, Italy*

^h*Università di Genova, Genova, Italy*

ⁱ*Università di Milano Bicocca, Milano, Italy*

^j*Università di Roma Tor Vergata, Roma, Italy*

^k*Università di Roma La Sapienza, Roma, Italy*

^l*AGH - University of Science and Technology, Faculty of Computer Science, Electronics and Telecommunications, Kraków, Poland*

^m*LIFAELS, La Salle, Universitat Ramon Llull, Barcelona, Spain*

ⁿ*Hanoi University of Science, Hanoi, Vietnam*

^o*Università di Padova, Padova, Italy*

^p*Università di Pisa, Pisa, Italy*

^q*Università degli Studi di Milano, Milano, Italy*

^r*Università di Urbino, Urbino, Italy*

^s*Università della Basilicata, Potenza, Italy*

^t*Scuola Normale Superiore, Pisa, Italy*

^u*Università di Modena e Reggio Emilia, Modena, Italy*

^v*H.H. Wills Physics Laboratory, University of Bristol, Bristol, United Kingdom*

^w*MSU - Iligan Institute of Technology (MSU-IIT), Iligan, Philippines*

^x*Novosibirsk State University, Novosibirsk, Russia*

^y*Sezione INFN di Trieste, Trieste, Italy*

^z*School of Physics and Information Technology, Shaanxi Normal University (SNNU), Xi'an, China*

^{aa}*Physics and Micro Electronic College, Hunan University, Changsha City, China*

^{ab}*Lanzhou University, Lanzhou, China*

[†]*Deceased*

Supplementary material for LHCb-PAPER-2019-005

This appendix contains supplementary material that will be posted on the public CDS record but will not appear in the paper.

Additional information on the $\chi_{c2}(3930)$ state

The $\chi_{c2}(3930)$ meson was first observed by the B-factories [?, ?] in the reaction $\gamma\gamma \rightarrow D\bar{D}$. The LHCb results for the mass and natural width of this resonance are compared to the B-factory values in Fig. 1. The mass measured here is 2σ lower than the world average whilst the natural width is 2σ higher.

The B-factories also reported evidence for a second state, the X(3915), that decays to $J/\psi \omega$ [?, ?, ?, ?]. The Review of Particle Properties [?] gives the mass of this state as

$$m_{X(3915)} = 3918.4 \pm 1.9 \text{ MeV}/c^2.$$

Based upon an analysis of one-dimensional angular distributions [?] and the assumption that a $J^{PC} = 2^{++}$ state is produced only with helicity ± 2 , as is expected for a pure charmonium state, the X(3915) was assigned spin-parity 0^{++} . A natural interpretation would then be that it is the $\chi_{c0}(2P)$ state. However, as discussed in Refs. [?, ?, ?], this assignment is problematic since the natural width of the $\chi_{c0}(2P)$ state is expected to be larger. In addition, the $\chi_{c0}(2P)$ state should have a large branching fraction to $D\bar{D}$ final state whereas there is no evidence for the X(3915) state decaying to open charm. Reference [?] proposes that the X(3915) and the $\chi_{c2}(3930)$ states are the same state with spin-parity assignment 2^{++} . This requires that the zero-helicity amplitude dominates due to a significant non- $c\bar{c}$ contribution to the wave function. The Belle collaboration has subsequently observed another state, $\chi_{c0}(3860)$, which has a large natural width and decays to $D\bar{D}$ final state. This is a better candidate to be the $\chi_{c0}(2P)$ state [?]. The question of the nature and existence of the X(3915) state remains open. It is interesting to note that the value of the mass measured here is roughly midway between the values the PDG quotes for the $\chi_{c2}(3930)$ and the X(3915) states. Further studies are needed to understand if there are one or two distinct charmonium states in this region.

Additional information on the $\psi(3770)$ mass

Figure 2 summarises the measurements of the $\psi(3770)$ mass used by the PDG to calculate its average. Our measurement is in good agreement. The PDG average does not include the BES-II measurement [?, ?, ?],

$$m_{\psi(3770)} = 3772.0 \pm 1.9 \text{ MeV}/c^2,$$

given in Ref. [?] since it does not include the effect of interference between resonant and non-resonant $D\bar{D}$ production. The PDG average and our measurement also agree with the analysis of available e^+e^- cross-section data in Ref. [?]

$$m_{\psi(3770)} = 3779.8 \pm 0.6 \text{ MeV}/c^2.$$

The PDG also quotes a fit value that includes precision measurements of the mass difference between the $\psi(3770)$ and $\psi(2S)$ states made by the BES collaboration [?, ?, ?].

$$m_{\psi(3770)} = 3773.13 \pm 0.35 \text{ MeV}/c^2.$$

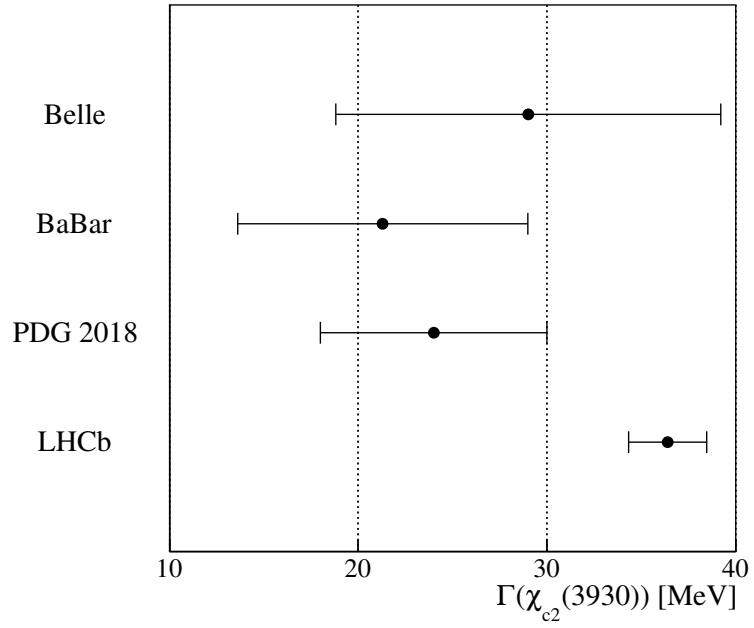
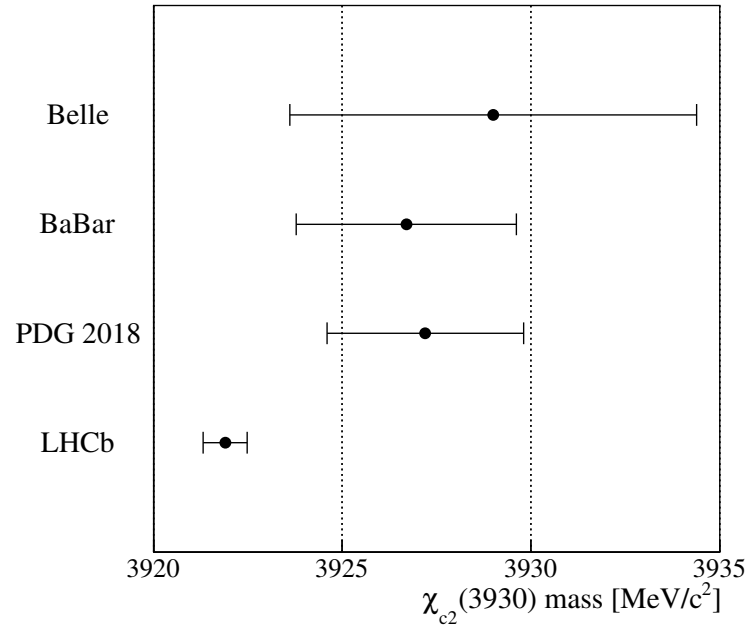


Figure 1: Measurements of the $\chi_{c2}(3930)$ (top) mass and (bottom) width by the Belle [?] and BaBar [?] collaborations together with the average calculated by the PDG [?] and the LHCb measurement.

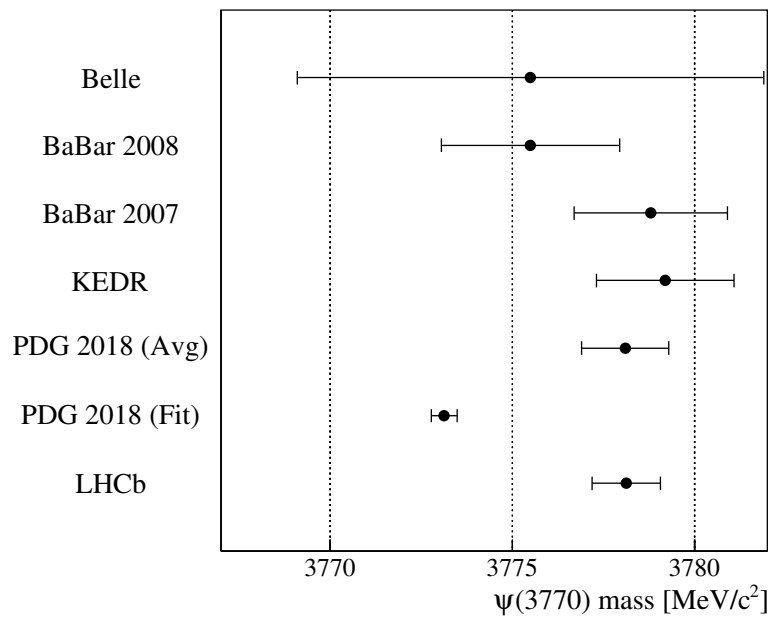


Figure 2: Measurements of the $\psi(3770)$ mass by the Belle [?], BaBar [?, ?] and KEDR [?] collaborations together with the average calculated by the PDG [?] and the LHCb measurement. The measurements are ordered according to decreasing total uncertainty, which is the sum of statistical and systematic uncertainties in quadrature. The PDG fit value is also shown.